culation by Scalapino and Marcus.[11] A more complete understanding of H_{TM} and its inherent limitations should now be possible using the "first-principles techniques" of Duke, Kleiman, and Stakelon.[14]

A typical result of this theory is shown in Fig. 1.

[1]J. Bardeen, Phys. Rev. Lett. **6**, 57 (1961).
[2]P. K. Tien and J. P. Gordon, Phys. Rev. **129**, 647 (1963).
[3]R. C. Jaklevic and J. Lambe, Phys. Rev. Lett. **17**, 1139 (1966).
[4]J. Lambe and R. C. Jaklevic, Phys. Rev. **165**, 821 (1968).
[5]A. A. Abrikosov, Physica (Utr.) **2**, 5 (1965).
[6]A. A. Abrikosov, L. P. Gorkov, and I. E. Dzyaloshinski, *Methods of Quantum Field Theory in Statistical Physics* (Prentice Hall, Englewood, Cliffs, N.J., 1963).
[7]C. B. Duke, Solid State Phys. 23 (1969).
[8]G. M. Eliashberg, Zh. Eksp. Teor. Fiz. **39**, 1437 (1960) [Sov. Phys.-JETP **12**, 1000 (1961)].
[9]D. J. Scalapino, J. R. Schrieffer, and J. W. Wilkins, Phys. Rev. **148**, 263 (1966).
[10]W. L. McMillan, Phys. Rev. **167**, 331 (1968).
[11]D. J. Scalapino and S. M. Marcus, Phys. Rev. Lett. **18**, 459 (1967).
[12]A. H. Dayem and R. J. Martin, Phys. Rev. Lett. **8**, 246 (1962).
[13]C. A. Hamilton and Sidney Shapiro, Phys. Rev. B **2**, 4494 (1970).
[14]C. B. Duke, G. G. Kleiman, and T. E. Stakelon, Phys. Rev. B **6**, 2389 (1972).

PHYSICAL REVIEW B VOLUME 8, NUMBER 1 1 JULY 1973

Electromagnetic Properties of Point-Contact Josephson-Junction Arrays

T. D. Clark

School of Applied and Engineering Physics and Laboratory for Atomic and Solid State Physics, Cornell University, Ithaca, New York 14850

(Received 16 October 1972)

The interaction of point-contact Josephson-junction arrays with electromagnetic fields, both self-generated and externally applied, is considered. Data are presented which suggest that such point-contact arrays can enter a "correlated" state in which the voltage drops at eacn of the junctions across the array equal the Josephson value $\hbar\omega_0/2e$ or some multiple or submultiple of this value. The use of these and other types of weak-link arrays as radiation detectors is discussed.

I. INTRODUCTION

Some years ago, Zimmer[1] reported the interaction of microwaves with superconducting tin films deposited on a rutile substrate and situated in a microwave cavity. The response of one or two of his samples appeared to follow that expected for a single Josephson weak link placed in a microwave cavity. It seems likely that these particular film samples were thin enough to be partially agglomerated. Zimmer interpreted his results in terms of a "granular" film[2,3] consisting of a kind of random array of weak links formed where the agglomerates of tin touched one another. Zimmer's data suggested that a large number of Josephson weak links connected by superconducting paths could be coupled together coherently. Similar behavior has been noted recently by Saxena *et al.*[4] and Warman *et al.*[5] for compressed superconducting powders. With the advantage of hindsight, it seems that Zimmer's granular film, situated as it was in a region of intense E field in a microwave cavity, was forced into over-all synchronization by the applied electromagnetic field. As Anderson[6] has stressed, the Josephson relationship between chemical potential and frequency is perfectly general, no matter what the particular physical process by which the relative phase changes with time. To restate Anderson's opinion, there appears to be no physical reason why almost any such motion should not be forced into essentially perfect synchronization, given a large enough applied signal.[7-9] On the assumption that such a situation could exist in Zimmer's films, we proposed what, in some respects, formed a model of a granular superconductor.[10] Our model system was based on the bubble-raft principle.[11] We chose to make arrays of uniform-diameter superconducting spheres, anticipating that where the spheres touched, Josephson weak links of very small cross-sectional area would be formed. This allowed us to make large numbers of weak links in a very simple way. Also, it appeared that planar arrays, at least, could easily be coupled to external microwave fields. All our experiments involving the interaction of arrays with electromagnetic fields, whether self-generated or applied, were performed on planar arrays of 1-mm-diam tin or niobium spheres.

Experimentally, synchronization of single Josephson weak links has been found to dominate over fluctuations at very low power levels.[12,13]

Both from our own observations and according to Taylor,[14] microwave-induced current steps have been observed in the I-vs-V curves of point-contact junctions when irradiated with as little as 10^{-10} W of X-band radiation ($E \sim 2\times10^{-4}$ V/cm), as measured at the top of the cryostat waveguide.

As an antenna system, two touching spheres approximate quite closely to an infinite biconical antenna with infinitely variable cone angle.[15,16] Consequently, touching spheres should serve as a relatively efficient structure for launching a TE wave from a very low-impedance source such as a Josephson point-contact junction.[17] The field distributions in the vicinity of a planar array of touching spheres are obviously more complicated than for a simple biconical antenna. However, to obtain an order-of-magnitude value for the field strength, we can take the simplest case of one junction radiating into free space. According to the literature,[18] point-contact junctions can, when situated in a resonant cavity and voltage-biased close to a cavity resonance frequency, radiate 10^{-10}–10^{-9} W of microwave power. In the case of a point-contact junction formed between two touching spheres it seems reasonable to assume that the aperture width L for the antenna system is approximately the sphere diameter d. Hence, even for emitted radiation with a free-space wavelength λ as short as 1 mm, another receiving antenna within a distance of 0.5 mm, equal to the lattice spacing for a close-packed array of 1-mm spheres, will still be well within the near-field region of the first antenna (conventionally taken equal to $2L^2/\lambda$[15]). At this distance and for the radiated power levels mentioned above, the maximum E-field strength turns out to be $\sim 1\times10^{-2}$ V/cm,[15,19] well in excess of the microwave field required to synchronize a single point-contact junction when situated in a waveguide. It appears, therefore, that two or more point-contact junctions, coupled to the same cavity mode, and placed within distances $\lesssim 1$ mm of one another should interact strongly enough to mutually synchronize their respective phase-time motions. A regular planar array of touching superconducting spheres may be self-resonant,[20] i.e., the array may have internal modes of oscillation due to its spatial periodicity. Conceptually, however, the interaction of an array of radiating point-contact junctions with an external cavity is easier to handle. For either case, the presence of a suitable resonant structure will serve to enhance radiative feedback and hence self-synchronization of the array. With an external cavity available, the radiation from one junction can be fed to all the other junctions in the array via the cavity. In such a point-contact array it is highly improbable that the normal-state resistances of the contact regions between the spheres should all be the same. However, if the array is fed from a single voltage source, through plane parallel electrodes at each end of the array, there should be a tendency for all the dc voltages across the individual junctions in the array to be pulled to the same value. The degree of voltage pulling will, of course, depend on the strength of the radiation fields and the degree of feedback.

Tilley[21] has developed a theory for arrays of superconducting weak links. In this theory it is assumed that self-synchronization of an array can occur through the interaction of the array with the common radiation field in the cavity. This self-synchronization process, which must be strongest near to a cavity resonance, acts so as to make the voltage drops across all the weak links the same. Tilley chose the simplest possible model of an array, namely, M junctions in series, connected by bulk superconducting paths, fed from a single voltage source, and interacting with a single external cavity mode. The current J passing through each weak link is the same but the normal-state conductivity and coupling to the radiation field are assumed to vary from weak link to weak link.

Tilley assumed that there are two distinct states in which the array can find itself. It can be in what we shall call an "uncorrelated" state, in which each weak link in the array has its own unique dc voltage V and interacts with its own photon of frequency $\omega = 2eV/\hbar$. On the other hand, the array can find itself in a "correlated" state, in which all the dc voltages are equal to the Josephson value $V_0 = \hbar\omega_0/2e$ or some multiple or submultiple of this value. We shall refer to an array in this state as being in the single-frequency condition. In this state the weak links interact with a common radiation field.

For an array operating in the single-frequency condition, Tilley predicts that the photon density n in the cavity is given by

$$n = G^2/[(\Omega-\omega)^2+\Gamma^2]\,, \tag{1}$$

where $\omega/2e$ is the dc bias across any weak link ($\hbar=1$), Ω is the cavity resonance frequency, Γ is the cavity linewidth, and G describes the coupling of the array to the common radiation field.

In terms of the relative pair phase ϕ_m, radiation phase α_m, and coupling constant g_m to the radiation field at each weak link ($m=1$ to M) in the array, G is given by the expression

$$G^2 = \sum_m g_m^2 + \sum_{m\neq m'} g_m g_m' \cos[(\phi_m-\alpha_m)-(\phi_m'-\alpha_m')]\,, \tag{2}$$

with $\phi_m-\alpha_m$ determined self-consistently by

$$\sin(\phi_m-\alpha_m) = [J - S_m(\omega)]/2g_m n^{1/2}\,. \tag{3}$$

Here, $S_m(\omega)$ represents the quasiparticle background current.

The main features of the theory become much more apparent when all the weak links in the array are taken to be identical. Then $S_m = S$, $g_m = g$, and from Eq. (3), all the $\phi_m - \alpha_m$ terms will be the same. This leads directly to

$$G^2 = M^2 g^2 , \tag{4}$$

$$n = M^2 g^2 / [(\Omega - \omega)^2 + \Gamma^2] , \tag{5}$$

and the Hamiltonian for the system is given by

$$H' = \frac{-M^2 g^2 (\Omega - \omega)}{(\Omega - \omega)^2 + \Gamma^2} - \frac{2M^2 g^2 \Gamma}{(\Omega - \omega)^2 + \Gamma^2} \arctan \frac{\Gamma}{\Omega - \omega} . \tag{6}$$

As Tilley points out $n \propto M^2$ is the super-radiant property[22,23] of M coherent radiators. In this "super-radiant" state $|H'| \propto M^2$, which suggests that such a state should be favored over the uncorrelated state (where $|H'| \propto M$) for reasonably large variations in the properties of the weak links comprising the array. For very large M[1,4,5] ($\gtrsim 10^6$), gross differences between individual weak links should prove tolerable. One interesting feature of this theory is that for a linear array, super-radiance can occur for any values of α_m; the superconducting phase difference ϕ_m simply adjusts to ensure that the supercurrent is feeding maximum power into the cavity mode at each weak link. However, in two- (or three-) dimensional arrays there are obviously more restrictions on the modes that can be excited.

In the super-radiant state the array behaves essentially as a single weak link, with a coupling constant to the common radiation field of $G^2 = M^2 g^2$, and a supercurrent versus voltage characteristic that is scaled up in voltage by the number of weak links M, across the array between the electrodes. For nonidentical weak links this scaling factor will still occur, but the interference terms in Eq. (2) will act to reduce both G^2 and n.

An alternative model for a "coherent" state in weak-link arrays, in which the whole array behaves like a single weak link, has been proposed by Rosenblatt[24-26] and his co-workers. They propose that such an array may, at a certain temperature (less than the critical temperature T_c for the "bulk" grains making up the array), undergo a transition from a resistive state, caused by a phase slip, to a truly resistanceless state. They postulate that this "coherence" transition, brought about by phase ordering within the array, is the exact analog of the paramagnetic-ferromagnetic transition in the Ising model. As would be expected from a restricted analysis based on the Ising model, overall phase coherence is not predicted for linear arrays. This model is an appealing one, at least for the dc ($\omega = 0$) state, but the experimental data do not[24,25] seem to demonstrate adequately the existence of this state. In particular, for the resistance-versus-temperature transitions, it should be noted that neither the Rosenblatt-group data nor ours[10,27] were derived from genuinely four-terminal measurements. It is therefore difficult to discuss in a meaningful way a truly resistanceless state. Also the anomalously low transition temperatures recorded for Nb and Ta arrays may well be due to the effects of impurities in the contact regions.[28]

The analogy with spin-ordered systems may provide a basis for the theoretical investigation of weak-link arrays at finite voltages. On the Rosenblatt model, the lowest-energy excitations from the ground state of an array of weak links could conceivably be "phase-wave" excitations by analogy with spin waves in ferromagnetic systems.

The data presented in this paper show that under suitable circumstances point-contact Josephson-junction arrays of the type discussed above can enter a single frequency, presumably super-radiant, state in which all the Josephson junctions in the array oscillate at the same frequency and in phase with one another. Thus, in Sec. IV we describe the manner in which a point-contact junction array can be made to self-synchronize by interaction with an external electromagnetic cavity. The alternative method of collectively synchronizing point-contact arrays, by application of an external rf field, is described in Sec. VI. In both cases it appears that the array acts in a very similar fashion to a single junction except that the voltage at which a self-induced or rf-driven current step occurs changes from $\hbar\omega/2e$ to $M\hbar\omega/2e$, where M is the number of junctions across the array between the electrodes. This is, of course, just the condition for super-radiance proposed by Tilley.[21]

II. FABRICATION OF WEAK-LINK ARRAYS

Ideally, it would have been best to start experimental work on carefully defined thin-film microbridge arrays. However at the time we started our investigations neither the technology nor the money were available to initiate a development program on microbridge arrays. We therefore kept to sphere arrays, which could be arranged in one, two, or three dimensions. Whatever the dimensionality of the array, a rigid support structure and mechanically adjustable electrodes were always required. For electromagnetic studies, at least, the support structure needed to be reasonably transparent in the far-infrared and microwave regions of the spectrum.

Our early studies were performed on two- and three-dimensional arrays of spheres mounted in structures machined out of lucite. Considerable improvements were subsequently made in the de-

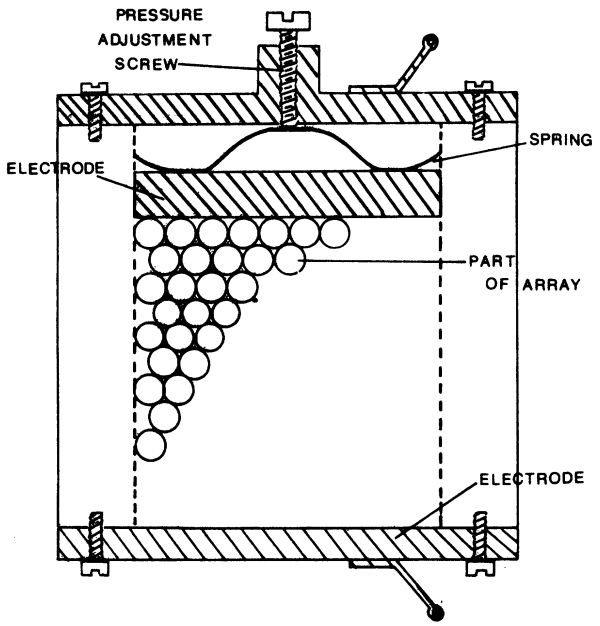

FIG. 1. Schematic of a two-dimensional array in its mounting structure.

sign and construction of mounting structures, but, in general, there were always some small imperfections in the array. From Tilley's analysis it appears that provided there is a continuous superconducting path connecting all the weak links in the array, the superconducting phase ϕ_m can adjust to ensure a maximum array correlation energy. A small number of imperfections is probably acceptable. Presumably, in real two- or three-dimensional arrays an open circuit between two spheres is simply bypassed. Also any large area contact between two spheres (i.e., a strongly coupled linkage) should function as a bulk superconductor. Although we cannot expect such contacts to take part in radiative processes, they can still serve to carry the phase information to the "active" contacts.

Electrical contact was made by means of plane parallel brass electrodes. In general, the electrodes were either silver or gold plated, gold being favored over silver for its resistance to atmospheric corrosion. One of the electrodes could be mechanically adjusted by means of a screw. This allowed the force on the array to be changed, and hence its resistance to be varied. Later versions of this two-dimensional array holder incorporated a spring mounted adjustable electrode, depicted schematically in Fig. 1.

The electrical measurements made on these arrays were not properly four terminal. However, the errors involved were small. The series resistance between the electrical leads at each end of the array holder and the end faces of the electrodes was negligible ($< 1\ \mu\Omega$ at room temperature). The only other series resistance involved is the contact resistance between the line of spheres adjacent to each electrode and the electrode itself. This resistance could not be avoided without using superconducting electrodes. At the time we were concerned with the properties of the weak links within the array itself; we did not want any confusion to arise from weak links formed at the electrodes. We therefore decided to use normal electrodes of brass. With the electrodes gold plated the contact resistance usually amounted to only a few percent (or less) of the normal-state resistance of the array. In microwave experiments on niobium-sphere arrays we were looking for constant-voltage current steps in the I-vs-V characteristic, and finally hit upon the solution of cladding the electrodes with a 1-mm thickness of tin or solder. When machined flat these "hybrids" made perfectly good electrodes. Furthermore, the tin or solder was so much softer than the niobium that relatively very large area contacts were made between the niobium spheres and the electrodes. This virtually eliminated the contact resistance problem.

The two-dimensional array holder was machined so that it was just large enough to allow an integral number of spheres, usually ten, to be contained across its width. The tin spheres used in the early experiments showed a variation in diameter of a few percent, so an absolutely accurate fit of the array to the array holder was not possible. In the later microwave experiments involving niobium-sphere arrays we were able to achieve a uniformity of 5 μm on 1 mm by careful selection of the spheres.

Although Tilley chose a linear array as his model system,[21] experimentally it is not the easiest of systems to get results from—at least for a reasonable long array of, say, ten spheres. Firstly, any open circuit stops the experiment completely. We found this occurred very frequently. We concluded that the trouble arose from the slight nonuniformity in the diameters of the tin spheres. The internal diameter of the tube holding the array has to be large enough to accommodate the largest of the tin spheres. Under pressure, the smaller spheres tend to ride up on the larger ones. This often led to the spheres jamming in the tube. In this situation the array was frequently found to be an open circuit. A two-dimensional array has more "give." With one electrode moveable, the array can rotate its axes slightly to accommodate any small differences in the diameters of the spheres and slight inaccuracies in the machining of the array holder. In practice, we found two- (and three-) dimensional arrays far easier to work with than linear arrays.

For the far-infrared experiments we chose PTFE as the material for the mounting structure. This is more transparent in the far-infrared and microwave region of the spectrum than Perspex.[29] It is also harder and better to machine than ordinary polythene. We later came upon "Epibond" which is a much superior material for the construction of array holders. It has a coefficient of expansion close to that for stainless steel (i.e., will match the contraction of the spheres quite accurately), is reasonably transparent to microwaves (10–120 GHz in frequency), and machines very well.

Except for the microwave experiments described in Sec. VI, all adjustments of array resistance were carried out either at room or liquid-nitrogen temperatures, but not *in situ* in the helium bath. We aimed at array resistances ~1 Ω at helium temperatures. Arrays with approximately this resistance were found to possess reasonable critical currents at low reduced temperatures (~few hundred μA). They were also of high enough resistance to be measured by our derivative plotter. Specimens with resistances much less than 1 Ω saturated the operational amplifiers used in the plotter, and so were not accessible to measurement.

III. dc PROPERTIES

The dc properties of arrays of tin spheres have been discussed in some detail in earlier publications.[10,27,43] All tin arrays showed a resistance-versus-temperature transition starting at the bulk critical temperature T_c for tin (= 3.72 K). A broad exponential tailing region was always observed below T_c. The tailing region was attributed to thermally activated phase slippage in the junctions making up the array.[10] The measured voltage at fixed measuring current appeared in every case to merge continuously into the noise. Careful examination of these resistive transition curves revealed that the top end of the curve, approaching T_c from above, was slightly rounded off. This effect was believed to be due to bulk superconducting fluctuations in the contact regions between the spheres.[27]

We measured the critical current as a function of temperature for Sn-Sn and Sn-Pb single contacts; also for two- and three-dimensional arrays of tin spheres. The diameter of the spheres used was in most cases 1 mm. We observed that weakly coupled Sn-Sn and Sn-Pb contacts (R_n from 0.1 to 1 Ω) follow the theoretical calculation of Ambegaokar and Baratoff[30] (AB) quite closely. In particular the two types of contact show completely dissimilar behavior near the transition temperature of the tin. J(Sn-Sn) approaches T_c linearly while the slope of J(Sn-Pb) becomes essentially infinite at T_c(Sn), as predicted by the AB theory. Close-packed arrays of Sn-Sn contacts (both two and three dimensional) follow the AB curve for a symmetric junction fairly accurately but the current at a given temperature is always slightly more than the predicted value. Since the spheres appear to consist of large crystals of tin the observed excess current may be due to gap anisotropy in the tin.[31] According to Ambegaokar and Baratoff, any inequality (i.e., anisotropy) in the energy gaps of the superconducting materials on each side of the tunnel barrier will show up as a positive deviation from the J-vs-T curve for a symmetric junction. Thus for a large ensemble of weak links, formed by superconducting tin spheres in contact, any gap anisotropy in the tin will presumably produce small positive deviations from the theoretical J-vs-T curve of the simple AB theory.

The normalized experimental curves are shown in Fig. 2 together with the theoretical curves approximating to the Sn-Sn contact ($\Delta_1 = \Delta_2$) and the Sn-Pb contact ($\Delta_1 = 0.4\Delta_2$).

In the normal state (i.e., for tin arrays, $T > 3.72$ K) the current-voltage characteristic is linear, at least up to 100-mV bias voltage. Immediately below T_c (bulk) "excess" currents appear—the current-voltage curve becomes convex upwards. The magnitude of these excess currents increases as the temperature decreases below T_c. Self-in-

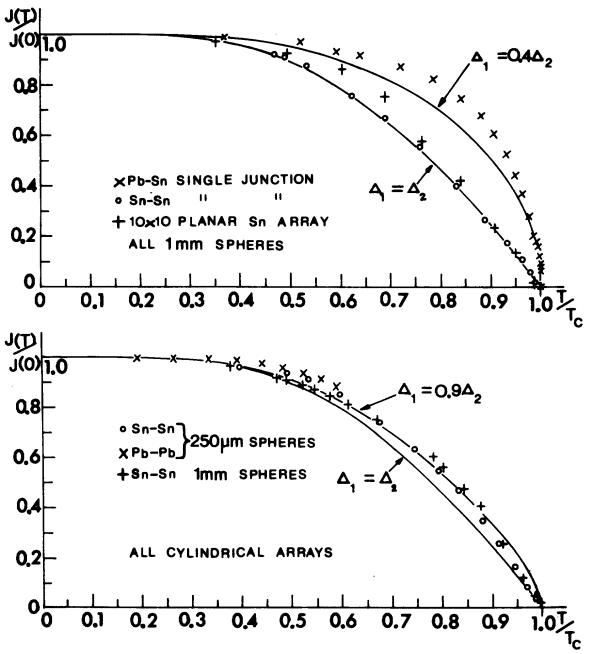

FIG. 2. Normalized zero-voltage supercurrent-vs-temperature plots for single Sn-Sn and Pb-Sn point-contact junctions and for various two- and three-dimensional (cylindrical) sphere arrays. Full curves are calculated from the Ambegaokar–Baratoff theory (Ref. 30) for various ratios of the energy gaps Δ_1 and Δ_2.

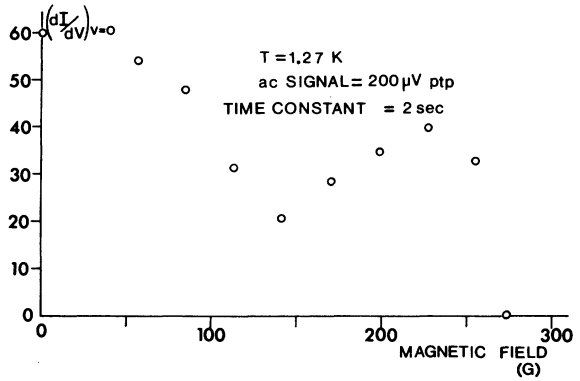

FIG. 3. Variation of the differential conductance of a 10×10 array of 1-mm Sn spheres at zero bias voltage as a function of magnetic field; dI/dV scale in arbitrary units.

duced structure does not appear in the characteristic until typically $T \lesssim 3.5$ K. The existence of excess dc in single-point-contact junctions is well known and is associated with the presence of ac Josephson currents in such junctions.[32–34,36] With regard to excess currents, the array I-vs-V curves appear to be scaled up in voltage (compared to a single contact) by the order of the number of contacts across the array between the electrodes. For cylindrical arrays of 1-mm tin spheres (approximately 9 cm long and 0.5 cm in diameter) excess currents usually continue out to at least 0.5 V, and for some arrays these currents could be seen at bias voltages of more than 1 V.

Applied magnetic fields spatially modulate the phase of the supercurrents flowing in an interferometer loop consisting of two or more junctions in parallel.[35] The smallest loop (or hole) in a close-packed planar array of 1-mm spheres is formed between three spheres in contact. This corresponds to a magnetic field periodicity ΔH for the loop supercurrent of $\sim 5 \times 10^{-4}$ G. It seems reasonable to assume that the maximum zero-voltage current has one period for the field change required to add one quantum of flux through each hole. Also there will be other faster oscillations related to the larger areas of the array (i.e., one periodicity for the flux through one hole, and one related to the flux through a line of holes).

With the available magnetic shielding we were not able to observe the small periodicities $\lesssim 10^{-4}$ G. Instead, we had to be content with measuring the slow period due to the magnetic flux threading the contact regions. We monitored the critical current or dynamic conductance of a close-packed planar array of 1-mm tin spheres as a function of a magnetic field applied normal to the plane of the array.

Figure 3 shows a typical set of results for this field measurement. The periodic variation of the dynamic conductance with applied magnetic field can clearly be seen. The zero-voltage supercurrent (or dynamic conductance dI/dV) does not fall to zero in the region of the minima. Such shallow field modulation of the critical current is quite typical of point contacts.[35] Each contact may contain several weak-link bridges with an enclosed area for flux between them. However, we observed no field modulation of I_c which could be attributed to multiple linkages in the contacts.

The field periodicity extrapolated to $T = 0$ K is 155 G. This corresponds to an enclosed area for flux of $\sim 10^{-9}$ cm^2 per contact; that is, if we assume that the $(dI/dV)_{v=0}$-vs-H curve represents an averaged-out pattern for all the Josephson point-contact junctions in the array. For some arrays, field periodicities as large as 250 G were recorded. The field-modulation curves cut short at the critical field (H_c) of the bulk tin. This is due to the tin spheres themselves going normal. H (cutoff) shows the usual

$$H_c \approx H_0(1 - t^2)$$

dependence, where $H_0 = H_c$ at $T = 0$ K and $t = T/T_c$. From our data, H (cutoff) at $T = 0$ K, extrapolated from the higher-temperature values, is 302.8 G, close to the bulk critical-field value for tin.

The zero-temperature value of the magnetic field penetration depth λ in tin is 510 Å.[36] The contact region is, however, very disordered and from our measurements of fluctuation effects in arrays of tin spheres above T_c (bulk), we estimate the electronic mean free path l_e in the contact region to be $\lesssim 10$ Å. Since λ varies with l_e,[37] it appears that we should take $\lambda_{\text{contact}} \sim 2\lambda_{\text{bulk}} \simeq 1000$ Å. The enclosed area for flux in the contact region $\sim 2\lambda \times$(width of contact). From the maximum field periodicity of I_c we estimate the contact regions to be 0.4 μm^2. This seems to be about the right size for weak-link systems.

IV. ac PROPERTIES OF POINT-CONTACT ARRAYS: SELF-SYNCHRONIZATION

Given enough care, a single point contact in a cavity can be made to feed back on itself to produce current peaks in its current-voltage characteristic.[18] These current peaks will occur at certain discrete voltages corresponding to the resonances of the cavity. When the junction is current fed the peaks are seen as "shouldered" steps. With weaker coupling between cavity and junction (or more power dissipation) the steps smear out and become no more than bumps on a rising current background. This is, of course, what we would expect for a Lorentzian curve of small amplitude superimposed on the current-voltage characteristic. When microwave radiation of sufficient intensity,

and at a frequency ω close to that of the cavity resonance, is fed into the cavity, the junction-cavity system can be forced to oscillate at the frequency of the applied microwaves. The current step in the I-vs-V curve of the junction is pulled in voltage to the value $V = \hbar\omega/2e$ by the applied microwave field. Structure similar to that found for single junctions in cavities was always observed in the current-voltage characteristics of arrays of weak links, both with and without a well-defined resonant cavity present. This structure, which was assumed to arise from the nonlinear interaction of the array with its own radiation field, was subsequently identified with the existence of a single-frequency super-radiant state.[21] The data presented in this section appear to justify this assumption.

Figure 4 shows an example of self-induced structure without an obvious resonant cavity. Most of the structure in this I-vs-V curve is easy to discern. The square array, which consisted of a 5×5 plane of 1-mm niobium spheres, was mounted in a holder made of Epibond and fused quartz. The whole system, array plus holder, was situated inside an X-band waveguide, as depicted in Fig. 4.

There are forty possible weak-link contacts in the array (including those parallel to the electrodes) so it seems unlikely that they are all being driven normal independently at different values of the bias current. If this were the case, the current-voltage characteristic would look far more complicated than it in fact does. In our experience, most single point-contact junctions show a fairly sharp transition from the superconducting to the resistive superconducting state. Accordingly, an "uncorrelated" array should show many distinct switching regions, one for each independent contact going resistive. This does not seem to be the case in Fig. 4. Large superconducting contacts (with I_c's $\gg 1$ mA) display pronounced switching behavior, often accompanied by hysteresis.[38] This is often seen in the characteristics of arrays which have been subjected to considerable pressure (I_c's $\gg 1$ mA). However, in Fig. 4 there is no switching behavior nor is there any sign of hysteresis. Most probably the structure arises from the weak interaction of the whole array with some resonant structure. Whether the resonances are internal, due to the periodicity of the array, or external, is a matter of conjecture. Certainly, with such large areas for enclosed flux between the junctions in the array, we do not consider that the observed structure can be associated with the low-voltage structure mentioned by Clarke and Fulton.[39] This arises out of self-field effects in multiply connected junctions.

Invoking the single-frequency argument and assuming that there are four active junctions, we list in Fig. 4 the Josephson ac frequency and radiated free-space wavelength for each junction in the array. We postulate that the structure is caused by weak feedback from the array holder which presumably can act as a low-Q parallel-plate resonator. The dimensions of the array holder are included in Fig. 4. The high-voltage "harmonic" structure is smeared out considerably compared with the lower voltage structure. This feature is to be expected if the structure is cavity induced. Certainly most of the arrays we looked at showed this behavior.

When the array was placed centrally in a Fabry–Perot cavity so that the feedback was intentional, shouldered peaks were always seen. These usually formed easily recognizable harmonic and subharmonic series. An example of this behavior is shown in Fig. 5, for a close-packed planar array of 1-mm tin spheres. The first derivative (dI/dV vs V) is taken to make the structure more easily discernable. We assumed these structures were, as before, due to the nonlinear coupling of the array to itself, via the external Fabry–Perot cavity. We also assumed that if we voltage biased the array exactly at the minimum in dI/dV vs V, the array would be on resonance.

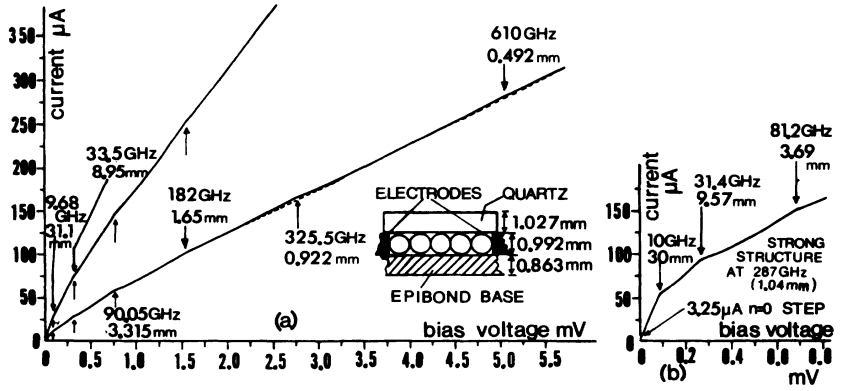

FIG. 4. Current-voltage characteristics for two 5×5 square arrays of nominally 1-mm Nb spheres. Inset in (a) is a sectional view of the array and array holder. The frequencies and wavelengths listed in (a) and (b) are calculated on the single-frequency argument. Mean-sphere diameter for array (a), 1.003 mm; for array (b), 1.029 mm.

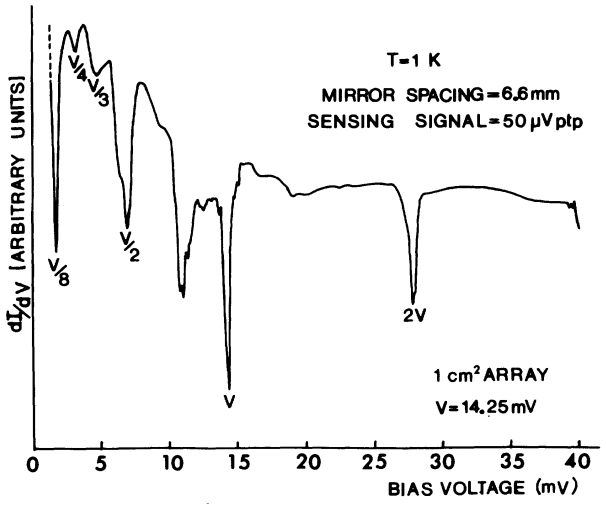

FIG. 5. Derivative curve for a planar array of 1-mm tin spheres placed centrally in a Fabry–Perot cavity. The array was 10 spheres wide and 14 spheres deep (between the electrodes). The sharp dip in the curve at 40 mV is the start of the 3-V minimum.

On our previous reasoning, if all the junctions in the array are coupled to a single cavity mode, the correlation energy across the array and the photon density in the cavity will go as M^2, where M is the number of junctions in the array. Since the arrays showed simple-harmonic and subharmonic structure in their current-voltage characteristics, we assumed that each shouldered peak reflected the interaction of the whole array with a single cavity mode. On resonance, i.e., at the minimum in dI/dV vs V, the radiation emitted by the array into the cavity should be a maximum. If the structure in I vs V is due to radiative feedback then moving the cavity off resonance by changing the distance between the mirrors should decrease the magnitude of the structure. We would expect the minimum in dI/dV vs V to become shallower as the array moved off resonance. It occurred to us that the array-cavity system would act as its own crude Fourier transform spectrometer if, at fixed bias voltage, the differential conductance dI/dV was monitored as a function of mirror spacing.

If the array is simply driven by the cavity and has no preferred resonant frequencies of its own, we should expect to see no periodic changes in dI/dV as a function of mirror spacing. The array-cavity system would be at resonance for all mirror spacings and we would expect to observe a shift in the self-induced structure toward lower voltages as the mirrors were moved apart, together with a slow decrease in $(dI/dV)_{V=V_{min}}$ as the mirror spacing and the Q of the cavity increased.[40] However, if the array does have preferred frequencies then changing the mirror spacing will change the coupling between the array and cavity very significantly.

According to Richards[41] the spectral response of a single resonant junction is broad for small values of the junction-cavity coupling constant Γ (at $\Gamma = 1$, the response is Lorentzian) but peaks very sharply in the range $2.0 < \Gamma < 2.9$. Since an array, if it is in the correlated state, will behave essentially as a single junction its response should be similar to that predicted by Richards. On this model $(dI/dV)_{V=V_{min}}$ should decrease very sharply when the mirror spacing is close to the resonant condition, i.e., when Γ is a maximum. In between resonances dI/dV should change relatively slowly with mirror spacing.

In practice, a close-packed planar array of 1-mm tin spheres was mounted in a PTFE holder and placed centrally between the mirrors of a Fabry–Perot resonator. The two mirrors were each 1 cm^2. The metal mirrors were gold plated to improve the surface conductivity. The arrangement of the cavity is depicted schematically in Fig. 6. As much as possible of the material surrounding the array was made of PTFE to avoid unintentional resonant structures. The mirror spacing of the Fabry–Perot could be changed from outside the cryostat by means of a drive shaft and gear system. The latter was coupled to a ten-turn helipot so that the voltage output from the helipot was proportional to the separation of the mirrors. The resistance of the array was set at room temperature.

The technique then adopted to search for radiation emitted from the superconducting array ($T \sim 1$ K) was to carry out a dI/dV-vs-V sweep and pause within one of the minima corresponding to a shouldered peak in I vs V. The pause facility on the derivative plotter allowed us to fix the voltage bias for periods $\gtrsim 30$ min for a total drift of only a few microvolts. The differential conductance of the array, at fixed bias voltage, was then plotted as a function of mirror spacing.

On the constant voltage mode (i.e., dI/dV vs V),

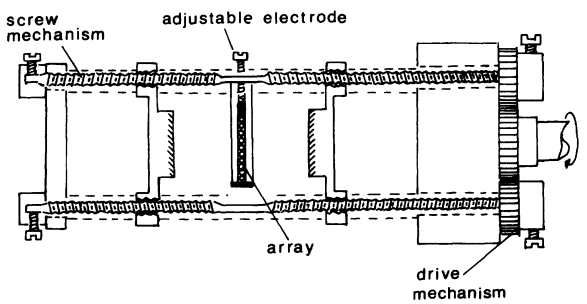

FIG. 6. Photograph and sectional drawing of the Fabry–Perot system used in the radiation-detection experiments.

the source impedance of the derivative plotted was approximately 3 mΩ for specimen resistances down to 1 Ω. The ac voltage modulation used in most of these experiments was 50-μV peak to peak. With a source impendance ~ 3 mΩ, we were therefore fairly confident of maintaining constant voltage bias within the range of the voltage modulation, for relatively large changes in the differential slope resistance. If the array response peaks sharply at resonance (as discussed above) the plot of $(dI/dV)_{V_{sp}}$ versus mirror spacing should show a series of sharp minima, where V_{sp} is the bias voltage at which the shouldered peak is observed. Each minimum corresponds to the resonant condition. Recently, this technique of self-detection has been used by Ulrich and Kluth[42] to observe radiation emitted by a single point-contact junction situated in a resonant cavity.

Periodic variations in the dynamic conductance of the array, at fixed bias voltages, were indeed

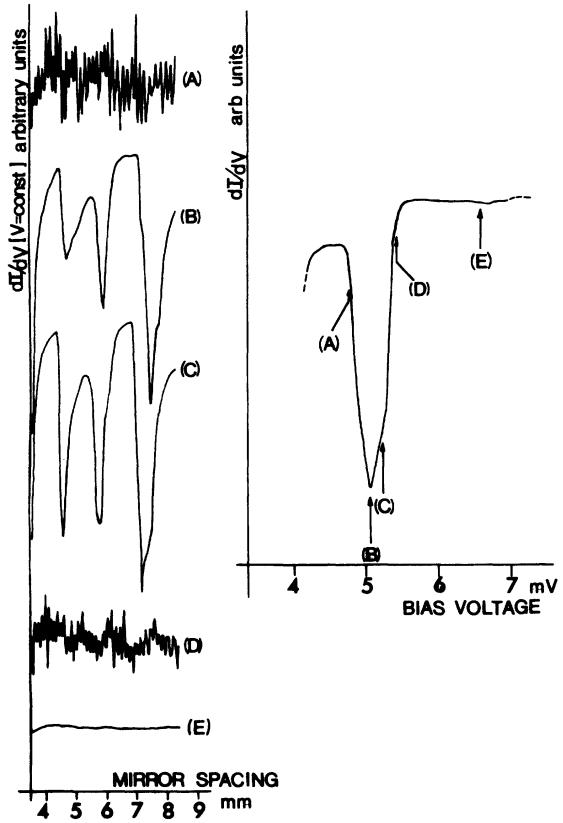

FIG. 7. Variation of dynamic conductance at fixed-biased voltage with mirror spacing for a 1-cm^2 array of 1-mm Sn spheres. Left-hand side shows mirror scans for the various bias positions A to E on the right-hand dI/dV-vs-V curve. The dynamic conductance is measured by applying a small ac voltage modulation at fixed dc voltage bias and synchronously detecting the ac signal produced (Ref. 41).

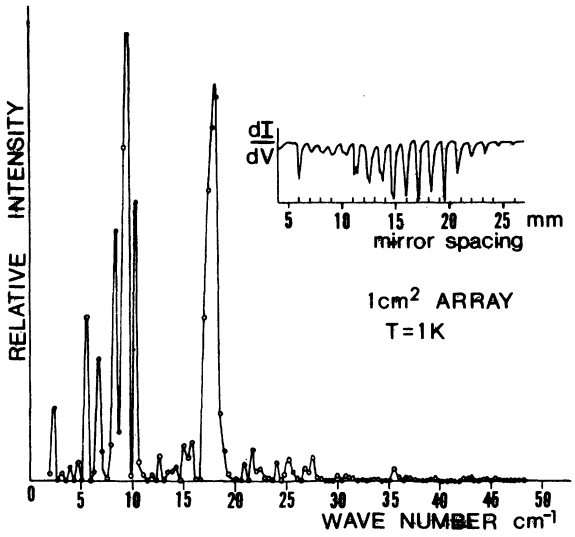

FIG. 8. Fourier transform of array interferogram shown in inset. This transform reveals that the radiation emitted by the array peaks sharply at 1.1 and 0.56 nm. Subharmonic structure, which is not well resolved can be seen below 10 cm^{-1}.

observed, but only in the region of the shouldered peaks in I vs V, i.e., the minima in dI/dV vs V. The results have already been discussed in an earlier paper.[43] Recently, Gregory and his coworkers[44] have confirmed these findings.

When the mirrors of the Fabry-Perot were very close together (~ 3 mm), periodicities as small as 100 μm were often seen. This was particularly noticeable when the array was voltage biased at the edges of a negative peak in dI/dV vs V, as illustrated in Fig. 7.

Since the spacing plot is a Fourier transform of the power spectrum of the emitted radiation, Fourier transforming this plot should provide at least an approximate spectrum of the radiation emitted from the array. Figure 8 shows the result of Fourier transforming a typical interferogram. As can be seen, the transform peaks very sharply at 1.1 and 0.56 mm, corresponding to the fundamental and second harmonic of the emitted radiation.

Generally, we found that only the fundamental and harmonic peaks varied in amplitude periodically, although Repici *et al.*[44] find that the subharmonic structure also shows this behavior. The dominant period in Fig. 8 is 1.16 mm, which, we assume, corresponds to the wavelength of the self-detected radiation. In other arrays, a dominant period close to 1 mm was regularly observed. The subharmonic minima showed changes in amplitude with change of mirror spacing, but usually no periodicity was apparent.

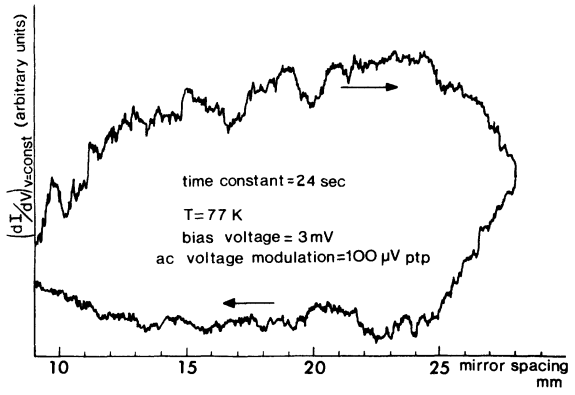

FIG. 9. Result of a mirror scan on the dynamic conductance at a fixed-bias voltage of 3 mV with the array at 77 K. The sensitivity on the conductance scale is 500 times greater than for the mirror scan in Fig. 8.

We could measure changes of differential resistance on our derivative plotter, and so were able to observe the change in the power drawn by the array from the voltage source as the differential conductance changed. In Fig. 8 the greatest $V^2(1/R_1 - 1/R_2)$ power difference between the maxima and the minima is $\sim 10^{-5}$ W. This close-packed array was 10 spheres wide by approximately 10 deep. If we take the number of active contacts M between the electrodes to be 100, and we assume a power output per junction $\sim 10^{-10}$–10^{-9} W, then the total "uncorrelated" power output should be $\sim 10^{-8}$–10^{-7} W. If, however, on resonance the array is in the correlated state, Tilley's argument[21] tells us that the power fed into the cavity (and stored in the common photon field) should go as M^2. On this basis, a correlated array ~ 100 junctions should produce $\sim 10^{-6}$–10^{-5} W of radiation. Since it is difficult to see where the V^2/R power difference between the maxima and minima should go but into the cavity, we take this 10^{-5} W as a reasonable order to magnitude value for the radiated power.

The maximum mirror spacing which could be accommodated in this system was just over 28 mm. After completing a full scan (usually from an initial 4–5 mm out to 28 mm and back again), it was found that although the amplitudes of the negative peaks in dI/dV vs V might have changed somewhat, their positions in voltage had not. Since the screw mechanism for the mirrors had some degree of backlash, this change in amplitude is not surprising. The backlash did not, however, affect the accuracy of the measurement on the outward or inward scan, taken separately.

It appeared that mirror scans could be made without disturbing to any noticeable extent the pattern of contacts within the sphere array. However, it was felt necessary to double check that the periodicity in $(dI/dV)_{V_{sp}}$ versus mirror spacing was not caused by some periodic mechanical movement—for example, the whole array holder-cavity system could be flexed periodically by the rotation of the drive shaft. If the flexion caused the pressure between the contacts to change this could lead to periodic changes in the current passing through the array. This explanation of the observed periodicity in $(dI/dV)_{V_{sp}}$ seemed very unlikely since there was no sign of such periodicity away from the negative peak regions in dI/dV vs V. However, if these negative peaks are, in fact, some kind of cavity-induced effect, it is conceivable that their amplitudes will vary in a very nonlinear way as a function of contact pressure (i.e., array current).

We decided to look for possible mechanically induced periodicities in a normal array but at greatly increased sensitivity. In Fig. 9 can be seen some of the results obtained for a normal array of 1-mm tin spheres at 77 K. The amplification is a factor of 500 times that used for the scan in Fig. 8. As can be seen, there is some small drift in dI/dV with mirror spacing, but no hint of periodicity. The same negative result was obtained for all applied voltages out to the maximum bias voltage possible on the derivative plotter (~ 30 mV). We concluded, therefore, that mechanical movements were not responsible for the observed periodicity in dI/dV as a function of mirror spacing. The only reasonable explanation remaining was that we were indeed observing the effects of electromagnetic radiation, emitted coherently from the array.

If in the region of the shouldered peaks in I vs V the array is "correlated" through the nonlinear interaction with its own radiation field, the correlation energy will be a maximum when the radiative feedback is optimized.

An array of weak-link oscillators has certain antenna properties which should affect its interaction with the Fabry–Perot system quite markedly. Judged as a stacked broadside array of in-phase dipoles[15] situated in a Fabry–Perot cavity, the array will have a maximum forward power gain for emission of radiation when the dipole spacing d is of the order of one-half the wavelength λ of the radiation. Conversely, the maximum radiative feedback from the cavity to the array will also occur when $\lambda \sim 2d$. For 1-mm-diam spheres arranged to form a close-packed array, λ should be close to 1 mm. This antenna argument looks to be the most likely explanation of our results. The operating wavelength would then be decided by the spatial periodicity of the array and not by the external resonator. If this is true, it should be possible to select the operating frequency of the array simply by changing the dipole spacing, viz., the sphere diameter. However, we experienced considerable

difficulties in preparing planar arrays of even 1-mm spheres so we did not attempt to move to smaller sphere diameters. These problems become rather trivial in microbridge arrays prepared photographically. The real problem is then to make good weak-link microbridges. In the special case where an external cavity is tightly coupled to the array, for example, when the mirrors of the Fabry–Perot are very close together, or in the transmitter-detector experiments referred to in Sec. V, the cavity may determine the operating frequency of the array.

Certain properties of the tin arrays we looked at suggest some kind of link up with the Riedel–Werthamer singularity[45,46] in the Josephson current at $V = 2\Delta/e$. First, for most of the arrays the fundamental conductance minimum in a given harmonic and subharmonic series occurs at a bias voltage very close to $M2\Delta/e$, where M is the number of junctions in series across the array between the electrodes. Second, the voltages at which the

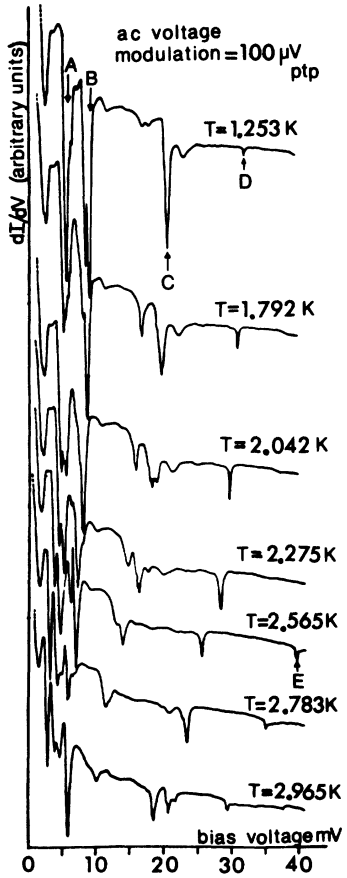

FIG. 10. Dynamic conductance curves for a 1-cm^2 array of 1-mm Sn spheres showing shift in the dynamic conductance minima to higher voltages as the temperature is decreased. Maximum scan voltage for this array resistance was about 40 mV.

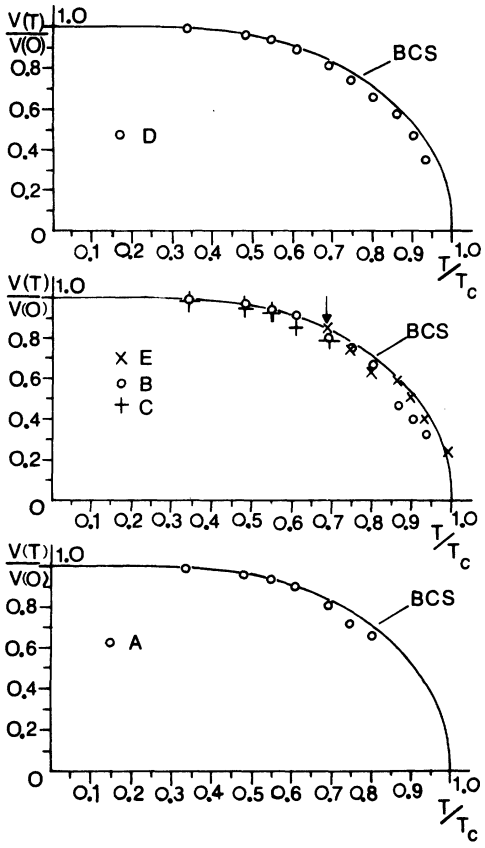

FIG. 11. Curves show the manner in which the dynamic conductance minima listed *A* to *E* in Fig. 10 vary their position in voltage as a function of temperature. Both voltages and temperatures are in reduced coordinates. Full curves show the BCS energy-gap-vs-temperature plot. Matching point denoted by arrow.

minima occur vary with temperature in a manner analogous to the energy gap in the BCS theory.[47] Figure 10 shows a set of derivative curves for a tin array approximately 1 cm^2 in area, taken at various temperatures below T_c(Sn). Clearly, the minima move out in voltage as the temperature is reduced below the transition temperature of tin (3.72 K).[48] Figure 11 shows the voltages at which some of the minima occur, plotted as a function of reduced temperature. The BCS plot of $\Delta(T)/\Delta(0)$ vs T/T_c is also included in the Fig. 11. Repici *et al.*[44] have also observed similar behavior.

If there is a connection, we may be observing images of the Riedel–Werthamer singularity at voltages $2\Delta/me$, where m is an integer (and, of course, at the harmonically related voltages $n2\Delta/e$). The free-space wavelength corresponding to the Josephson frequency at the tin gap voltage $2\Delta(0)_{Sn} = 1.1$ meV is 0.56 mm, so invoking the Riedel–Werthamer mechanism we are observing the fundamental and first subharmonic of the Riedel frequency, at equivalent free-space wavelengths of

0.56 and 1.1 mm, respectively. Which of the two points of view is correct we do not know, but probably the array (aerial) geometry governs the frequency of the radiation. However, the Reidel–Werthamer singularity may well determine the power output from the array. Tilley's super-radiance[21] argument tells us that the photon density in the cavity will go as the square of the sum of the individual contributions from each of the junctions in the array. The power radiated by each junction will naturally depend on the amplitudes of the ac's present. Hence in the region of the current singularity, the photon density in the cavity, and, by feedback, the correlation energy in the array should be enhanced considerably. On the antenna argument the array wavelength is ~1 mm (i.e., twice the dipole spacing), so it may be that the dominant cavity mode frequency arising from the geometry of the array is pulled towards the Riedel frequency, at least at low reduced temperature, where the two frequencies are comparable with one another.

The above experimental data provide strong evidence that the whole array-cavity system can, under suitable circumstances, oscillate predominantly at one frequency ω_0. The analog computer studies of Werthamer and Shapiro[33] indicate that Josephson-junction-cavity systems oscillate predominantly near the resonant frequency of the cavity whenever significant power is drawn from the junction into the cavity. If this is the case for an array in a suitable cavity, we can expect all the voltage drops to equal the Josephson value $V_0 = \hbar\omega_0/2e$, or some multiple or submultiple of this. Because of the extreme nonlinearity of the ac Josephson effect each junction can still radiate at frequency ω_0 whether its own voltage drop is $\hbar\omega_0/2me$, $\hbar\omega_0/2e$, or $n\hbar\omega_0/2e$, where m and n are integers. This is precisely what we appear to have observed in the neighborhood of the self-induced structure in the array I-vs-V curves.

V. GENERATION AND DETECTION EXPERIMENTS INVOLVING POINT-CONTACT JUNCTION ARRAYS

Following earlier experiments involving single point contacts we decided to look for radiation emitted from one array by means of a second array situated close by.[49] We showed first that arrays of point-contact junctions emit radiation only in the region of the self-induced structure in their current-voltage characteristics, and second that arrays can function both as broad and narrow band detectors of radiation. In these experiments we applied the techniques of broad and narrow band detectors described by Grimes *et al.*[50,51] and Richards and Sterling.[52] Grimes *et al.* showed that radiation incident on a point-contact junction decreased the zero-voltage critical current of the junction. By current biasing into the region of high differential resistance between the superconducting and resistive states, they were able to produce a very sensitive broadband detector. Their measurements always involved chopped radiation sources combined with phase-sensitive detection. Richards and Sterling demonstrated that a point-contact junction can also function as a narrow-band detector when biased into the region of a cavity-induced peak (step) in I vs V.

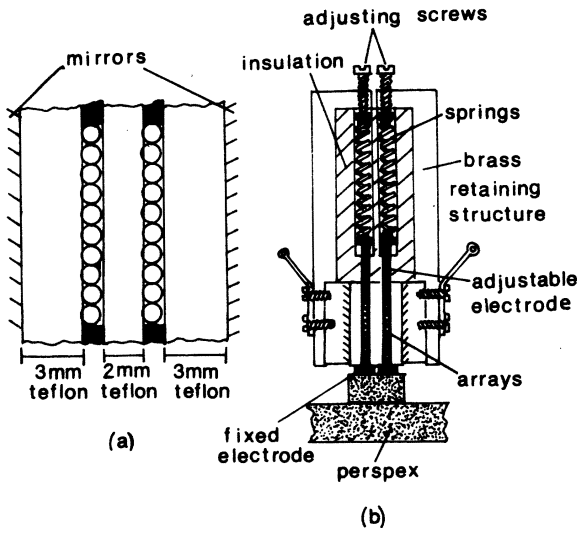

FIG. 12. (a) Dimensions and (b) sectional drawing of the double-array system used in transmitter-detector experiments.

As shown in Fig. 12 our experimental setup consisted of two 1-cm^2 (10×10) arrays of 1-mm-diam tin or niobium spheres. To improve their surface cleanliness the niobium spheres had been outgassed for 12 h at 1500 °C in a vacuum ~10^{-6} Torr.

The two arrays were contained within a PTFE structure and the whole arrangement was enclosed by two-plated brass mirrors, surface finished to ~1 μm. The two arrays were electrically isolated from one another, and the electrical leads were noninductively wound and screened in the usual manner. No attempt was made to optimize the radiation coupling between the arrays, for example, by altering the separation of the mirrors. It was assumed that the two arrays were at least reasonably coupled to one another. Contact pressure, and thus array resistance, could be varied by means of the spring-loaded adjusting screws shown. These acted on the upper rectangular plate electrodes, as illustrated in Fig. 13. All adjustments to the array resistances were made at room or liquid-nitrogen temperature. As usual, array resistances of at least 1 Ω were preferred because of the limited capabilities of our derivative plotter.

Typically, array resistances were in the range 1–3 Ω.

Following Grimes *et al.*[51] we current biased our detector array into the middle of the high-differential resistance region. Under these operating conditions we assumed that the array was acting as a broadband detector. Figure 13 shows the observed voltage changes at constant bias current amplified by a conventional dc amplifier, and plotted against the transmitter bias voltage. Also shown are the I and dI/dV-vs-V characteristics of the transmitter array. I vs V was plotted using a high-impedance current source. In the transmitter-detector experiment, however, the transmitter array was fed from a voltage source with an output impedance approximately a few mΩ for array resistances down to 1 Ω. Both the derivative curve and I vs V indicate that appreciable power is radiated only when the transmitter array is biased into the region of a shouldered peak (current bump) in I vs V. Insofar as we can assume that the detector has a broad-band response, it seems reasonable to identify these shouldered peaks with cavity resonances of the system. The correlation between the current bumps in the I-vs-V curve and the peaks in the detector response seems to be good. The detector is still responding weakly at about 70 mV, so assuming the transmitter is in the "correlated" state, it appears on the single-frequency argument that the transmitter is radiating at least up to 3500 GHz.

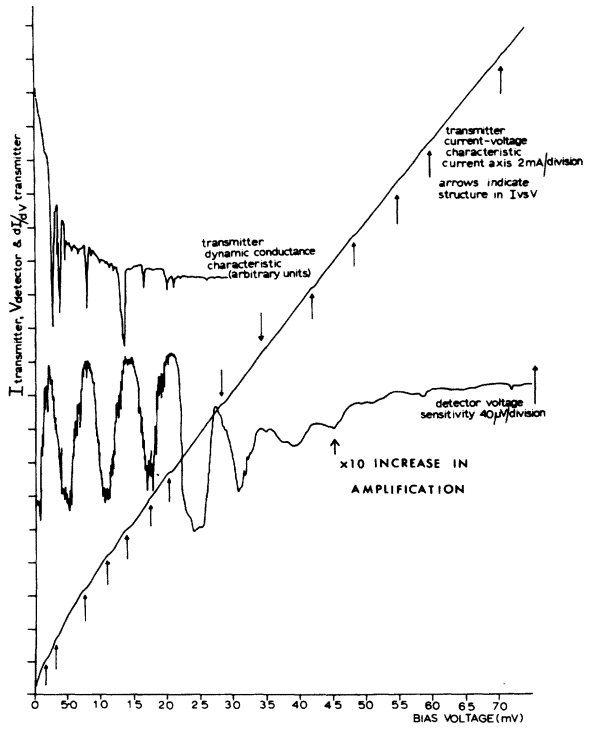

FIG. 13. Detector response as a function of transmitter voltage for a double-array system of 1-mm Sn spheres. Also shown are I vs V and dI/dV vs V of the transmitter. The detector is still responding weakly at 70 mV.

We can get some idea of the power radiated by the transmitter array if we assume that the zero-voltage supercurrent has a Bessel-function dependence[41] of the form

$$I_{\max} = I_1 J_0(2ev_0/\hbar\omega) ,$$

where J_0 is the zero-order Bessel function and v_0 and ω are, respectively, the amplitude and frequency of the incident ac. The observed depression of $I_1 \simeq 20\%$. This allows us to estimate v_0. The incident power is then given by $v_0^2/(\text{array impedance})$. If we take this impedance to be ~1 Ω and $\omega \simeq 300$ GHz, as seems reasonable on the single-frequency argument for the large response at $V_T = 14$ mV in Fig. 13, the maximum power detected by the array is $\sim 2\times10^{-7}$ W. On the single-frequency argument the detected power for the response peak at about 17 mV is of the same order. Using 1-mm niobium-sphere arrays in such transmitter-detector experiments, a maximum detected power $\sim 2\times10^{-6}$ W was recorded.[49] The detector response was checked as a function of transmitter voltage with the voltage leads connected to a 1-Ω resistor instead of the transmitter array. The response of the detector array was flat over the entire transmitter voltage range. Also the transmitter-detector experiments were tried above T_c(Sn), at 4.2 K. The response of the detector was once again flat over the whole range of the transmitter voltage.

Some of the structure observed in the current-voltage curve in Fig. 13 was repeated, at the same bias voltage, in the characteristics of almost all the arrays, both tin and niobium, we looked at. For example, the shouldered peak close to 2 mV was observed in most array characteristcs in the double-array experiments. Figure 14 shows in more detail the I-vs-V curve of the double-array system discussed in Fig. 13. The transmitter is clearly emitting radiation in this voltage region and appears to show a peak output at 2 mV (arrowed).

In some of the transmitter-detector experiments involving 1-mm niobium-sphere arrays, the coupling between the two arrays was strong enough to induce a constant current voltage step in the voltage-current step in the current-voltage characteristic of the detector array, at least over a certain range of transmitter bias current. Figure 15 shows such an induced current step. The step voltage is 1.96 mV. Both the transmitter and detector current-voltage characteristics displayed shouldered peaks close to 2-mV bias voltage. On

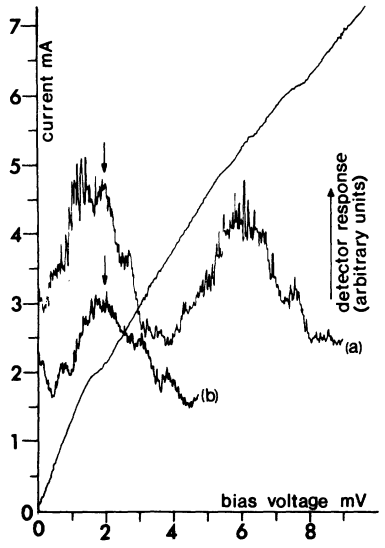

FIG. 14. Detail of detector response curve of Fig. 14 at low transmitter voltages. Also shown is I vs V for the transmitter array. The transmitter is clearly emitting radiation at around 2-mV transmitter bias (arrowed).

the single-frequency argument a step voltage of 1.96 mV means a frequency of 94.7 GHz or $\lambda_{\text{free space}} = 3.17$ mm for 10 contacts across the array. This wavelength is close to the separation distance between the two planes of point-contact junctions.

In a few of our experiments on double arrays extremely pronounced structure was observed in the I-vs-V characteristics of the arrays. The curve (a) in Fig. 16 is a particularly fine example. This low-voltage structure, which was plotted using a high-impedance current source, is very similar to the "Fiske" mode steps seen for thin-film Josephson tunnel junctions. Curve (b) of Fig. 16 shows our attempt to subtract the electrode contact resistance voltage. As can be seen, the first self-induced step is almost vertical. The 2-mV step, which is cut short in Fig. 16, is shown arrowed, as are possible subharmonics of this step. Similar, almost constant-voltage current steps were frequently observed in the I-vs-V characteristics of three-dimensional sphere arrays.

Figures 17 and 18 show the characteristic of Fig. 16 extended to higher voltages. With the electrode contact resistance voltage subtracted, further step structure is seen at 4.275, 13.13, 26.48, and 40.92 mV. These steps appear to form a harmonic-subharmonic series centered on the 13.13-mV step. On the single-frequency argument, the step at 40.92 mV implies that the array is still emitting radiation at a frequency of 2000 GHz. If the single-frequency argument is not invoked, and this step pattern is assumed due to the interaction of one junction with its surrounding cavity environment, extremely high operating frequencies must be proposed, in the range 20 000–35 000 GHz.

In curves (a) and (b) of Fig. 17 the "narrow-band" response[49,52] of the detector array is plotted for

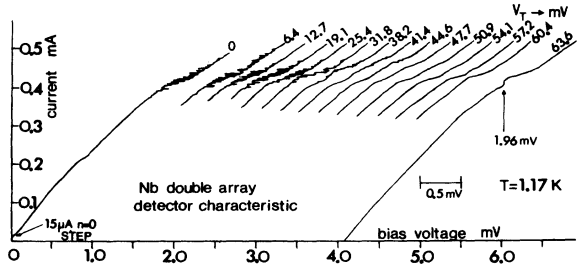

FIG. 15. Current-voltage curves for a 1-cm^2 detector array of 1-mm Nb spheres. As the transmitter voltage V_T (or current) is increased the small zero-voltage supercurrent is suppressed completely and the resonance structure close to 2 mV is stabilized as a constant-voltage current step.

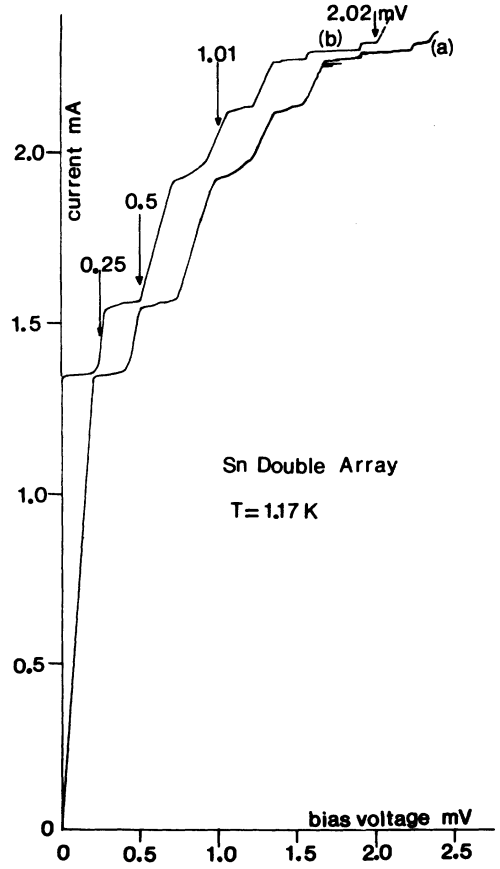

FIG. 16. (a) Pronounced structure in the current-voltage characteristic of a 1-cm^2 array of 1-mm Sn spheres used in transmitter-detector experiments. Curve (b) shows the attempt to subtract the contact-resistance voltage.

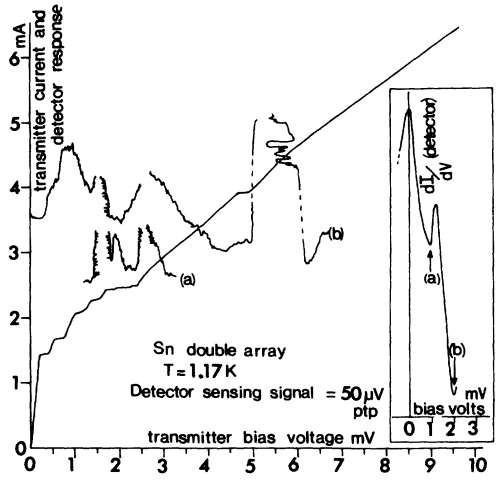

FIG. 17. I-vs-V curve in Fig. 16 extended to higher voltages. The "narrow-band" response of the detector array is also included; (a) and (b) refer to the two voltage biases chosen for the detector array. The detector derivative curve is shown inset. On some transmitter current steps the detector response was so strong that it tended to change discontinuously. Where this has occurred the response is shown with a break or as a dashed line.

the detector voltage biased into minima in its dI/dV-vs-V characteristic. The bias points are marked (a) and (b) in the detector-derivative-curve inset. Curve (b) appears to justify our assumption that the structure is I vs V is cavity induced. The response is particularly strong at the 2.02 and 4.275-mV steps.

VI. INTERACTION OF POINT-CONTACT JUNCTION ARRAY WITH MICROWAVE FIELD

In Secs. I and IV we presented theoretical arguments to justify the idea that an array of weak links, biased into the region of a cavity-induced peak in its current-voltage characteristic, oscillates predominantly at a single frequency ω_0. In this condition we postulated that the voltage drops across the array would be equal to the Josephson value $\hbar\omega_0/2e$, or some multiple $m\hbar\omega/2e$, or submultiple $\hbar\omega_0/m'2e$. Collective synchronization of a weak-link array by means of an externally applied microwave field should also be possible. The experimental results presented below indicate that such a synchronization process is feasible and that, once again, on a collectively driven constant-voltage current step, the array is in the single-frequency condition, with the voltage drop at each weak link across the array being the same.

It is now extremely well established that applied microwave fields can frequency modulate[7,53] the ac currents in a Josephson weak link biased at nonzero voltages. The outcome of the modulation process is the appearance of constant-voltage current steps at voltages given by $n\hbar\omega/2e$, where ω is the microwave frequency and $n=0, 1, 2, \ldots$. These steps, which provide a good qualitative test for the presence of ac Josephson currents, change in amplitude with the microwave voltage v_0 as the Bessel functions $J_0(2ev_0/\hbar\omega)$, $J_1(2ev_0/\hbar\omega)$, $J_2(2ev_0/\hbar\omega)$, ..., etc. If it is possible to synchronize a complete weak-link array by means of an external microwave field, constant-voltage current steps should be seen in the current-voltage characteristic of the array at voltage intervals of $M\hbar\omega/2e$. M, as before, is the number of weak links across the array between the electrodes. Under suitable circumstances and at certain microwave power levels synchronization was indeed observed, as has already been reported briefly.[54] Also, if the array is truly in the single-frequency condition, and the critical current of the array is suitably adjusted, the various orders of the microwave-induced current steps should change in amplitude with v_0 as would a single weak link, viz., as $J_0(2ev_0/\hbar\omega)$, $J_1(2ev_0/\hbar\omega)$, $J_2(2ev_0/\hbar\omega)$, ..., etc.

The obvious way to perform the experiment is to place a planar array in a waveguide and look for "correlated" current steps as the microwave power is increased. We required waveguides sufficiently large in section to ensure that a small array of 1-mm spheres placed in the guide would not disturb the field patterns unduly. We chose to investigate 5×5 arrays of 1-mm-diam niobium spheres centrally positioned in a 3-cm (~10-GHz) waveguide. We expected the 3-cm wave to be single moded (in the H_{10} transverse electric mode) until relatively close to the array (~1 cm). Ideally, we wanted the electric field vector to be aligned across

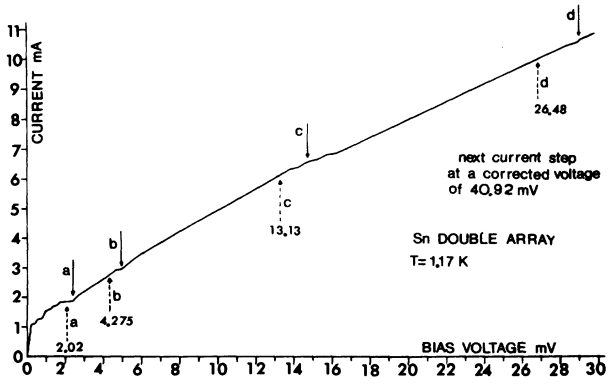

FIG. 18. Current-voltage characteristic of Figs. 16 and 18 extended to higher voltages. Corrected step voltages (with electrode contact-resistance voltage subtracted) denoted by broken arrows. Steps appear to form a harmonic-subharmonic series centered on 13.13 mV (635 GHz, or a free-space wavelength of 0.473 mm on the single-frequency argument for 10 contacts across the array).

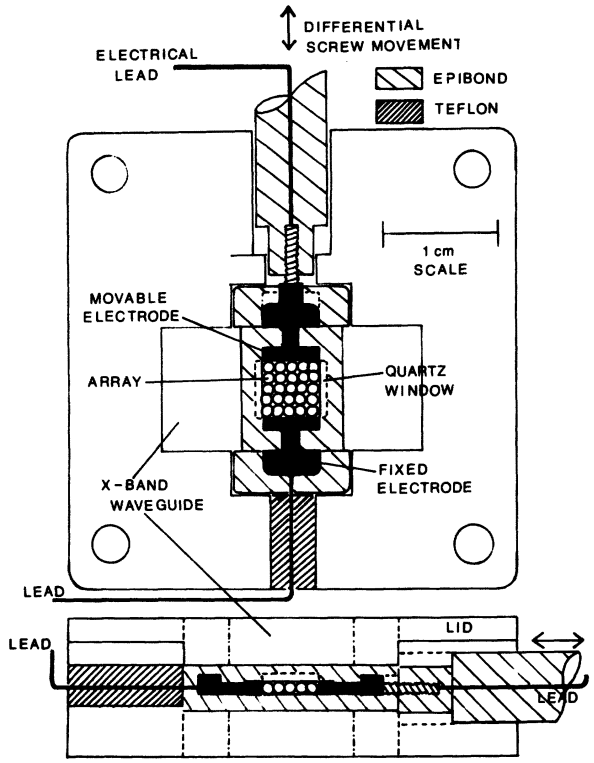

FIG. 19. Schematic of array mounting structure and pressure adjustment system used in microwave experiments on 5 × 5 square array of 1-mm Nb spheres.

the array at right angles to the plane parallel electrodes. As it turned out the obstruction caused by the array plus electrodes plus array holder did not seem too great. With a short-circuit plunger mounted below the array system, we measured standing-wave ratios ≥ 50 as the short circuit was moved towards the array.

Though conveniently small in area, such arrays were able to demonstrate correlation effects over a reasonable number of weak-link contacts, i.e., four weak links across the array between the electrodes. The arrays were either close packed or square, the change over being rather easy to achieve with such small arrays. In any one array we were able to select the diameters of the spheres to be within 5 μm of each other.

The array was mounted in an Epibond tray closed at both ends by plane parallel electrodes. These brass electrodes were either superfinished and then gold plated, or were tin plated to a depth of about 1 mm. The tin was then superfinished to produce a very flat face on the electrode. Niobium electrodes were also tried. These were always extremely difficult to machine to be exactly plane and parallel when situated in the array holder. The array holder was completed by means of a 1-mm-thick quartz window and the whole system was placed in an X-band waveguide.

The pressure on the array, and hence its resistance, could be varied by means of an externally controlled differential screw mechanism. With external gearing one turn of the (external) control knob was translated into a linear movement of a few microns. The resistance of the array (i.e., in the resistive state at a few millivolts bias) was usually set at about 1 Ω at 4.2 K. The array and array holder are shown in Fig. 19. A short-circuit plunger was mounted behind the array at $\frac{5}{4}$ of a guide wavelength (corresponding to the operating frequency) in an attempt to maximize the E field at the array.

Microwave power was generated by a Philips reflex klystron (type 2K25) with a maximum power output of > 20 mW at ~ 9 GHz. Modulation of the microwaves (up to 90%) was provided by a PIN Diode (Philips PM 7025X) mounted in a section of the waveguide system preceding the calibrated attenuators. A Hewlett-Packard model No. 432A power meter was used, in conjunction with a suitable thermistor mount (X486A), to measure the microwave power flowing through the system. The experiments were performed in a screened room, well filtered electrically from external disturbances. Considerable care was also taken to avoid ground loops.

The array and lower end of the waveguide were positioned well down in an open-ended mu-metal can, 14 cm in diameter and 50 cm long. This can was mounted in the interspace between the nitrogen and helium Dewars. A weak magnetic field could be applied normal to the array by means of a pair of Helmholtz coils situated in the nitrogen bath and enclosed by the mu-metal can. The coils were so placed that the array was central between them. A similar mu-metal can, but much larger (ϕ = 30 cm, length = 100 cm), could be used to enclose the whole lower end of the cryostat. With both cans in position the axial field near the bottom of the inner can was about 10^{-3} G.

Figure 20 shows a set of I-vs-V curves for a 5 × 5 square array at various levels of rf power. The steps are not truly vertical, presumably due to the effects of external noise[55,56] on the high-resistance (low-critical-current) array. However, the Josephson relationship $\hbar\omega = 2ev$ apparently still holds if the voltage intervals are measured from the midcurrent points of the steps. On this basis, the voltage between steps as measure on the −1-dB curve is 73.5 ± 2.4 μV, i.e., close to $4\hbar\omega/2e$ ($\hbar\omega/2e$ = 18.92 μV for ν = 9.15 GHz). Since M, the number of possible weak-link contacts across the array between the electrodes equals 4, it does appear that the whole array is being forced to synchronize with the microwave field. We have discounted weak-link contacts parallel to the elec-

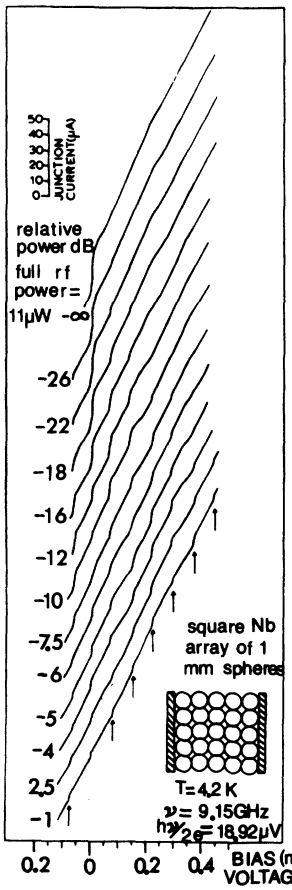

FIG. 20. Set of I-vs-V curves for a 5×5 square array of 1-mm Nb spheres at various levels of microwave power.

trodes, i.e., normal to the E field of the dominant H_{10} (transverse electric) mode in the rectangular waveguide.

Although the step amplitudes for the curves in Fig. 20 are not very large, we attempted to determine their dependence on rf voltage. Figure 21 shows the results obtained. As can be seen, the step amplitudes go through a series of maxima in a manner analogous to a single point-contact junction. The sharp drop to zero amplitude on the $n=1$ curve just beyond the first minimum coincides with the movement of a microwave power-dependent current bump through the $n=1$ step. Recent analog studies[57] of simple equivalent circuits representing a single Josephson weak link driven by an external microwave field indicate that good Bessel behavior for the microwave-induced steps will occur only when the parameter[58,59] $(\hbar\omega/2e)R^{-1}I_0^{-1}\gtrsim1$, where ω is the frequency of the microwave signal, R is the parallel resistance, and I_0 is the maximum zero-voltage supercurrent. If a correlated array of four weak links in series (our 5×5 array) can be similarly treated in terms of lumped components, we would expect the critical parameter to become $4(\hbar\omega/2e)R^{-1}I_0^{-1}$. For the data presented in Fig. 20, we find that $\hbar\omega/2e=18.92$ μV, $R_{\text{normal}}\simeq2.5$, and $I_0=12$ μA, giving $4(\hbar\omega/2e)R^{-1}I_0^{-1}\simeq2.4$.

The zero-voltage supercurrent step appears to show a small increase in amplitude ($\sim5\%$) at low levels of microwave power. Small superconducting bridges often show similar behavior, the so-called Dayem (or Wyatt)[8] effect, over a limited range of temperature.

Curves displaying constant-voltage current steps are usually plotted by current feeding the junction or array of junctions. Consequently, it is perfectly proper to plot the first derivative dV/dI vs V, since this function is obtained by using a constant current sweep. The current steps in I vs V show up as sharp minima in dV/dI vs V. Figure 22 shows such a derivative curve for a single Nb-Nb

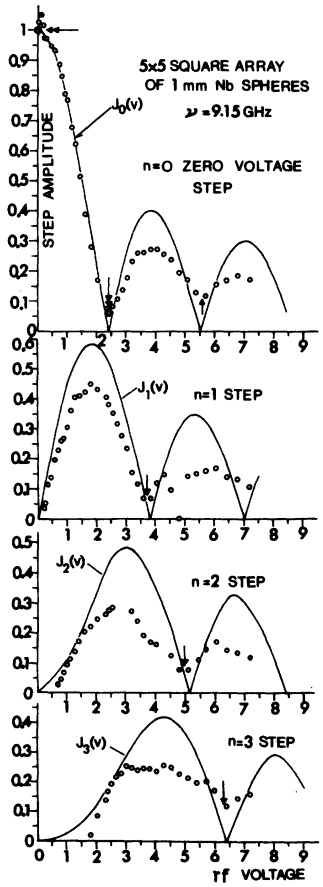

FIG. 21. Plots of step amplitude vs rf voltage for the steps $n=0$–3. The Bessel functions $J_0(v)$ to $J_3(v)$ are shown as full curves. The matching points for the four sets of data are shown ringed and marked by double arrows. The estimated positions of the minima in the experimental curves are marked by arrows. Unity on the voltage axis $\simeq1\times10^{-2}$ V/cm at the array.

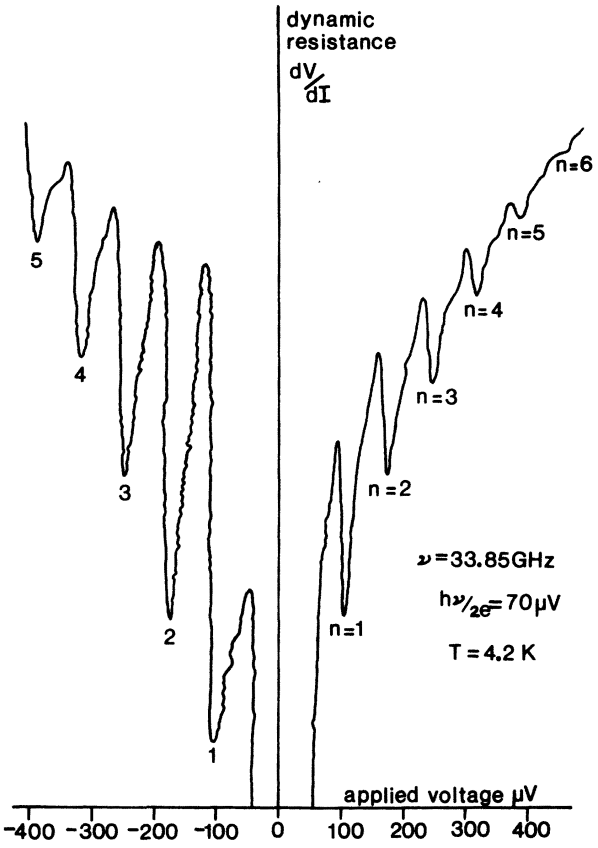

FIG. 22. Plot of dV/dI vs V for a single Nb-Nb point-contact junction exposed to 33.85-GHz radiation.

point contact exposed to 33.85-GHz radiation. The $n=0$ zero-voltage supercurrent step is cut off deliberately.

"Correlated" steps were also seen in the I-vs-V characteristics of close-packed arrays. Once again $M=4$. Since more detail could be obtained from the derivative curve, we plotted dV/dI vs V at various rf power levels. Some of these derivative curves are presented in Fig. 23. The sharp minimum at $V=0$ corresponds to the zero-voltage supercurrent of the array (I vs V is inset in Fig. 23). Higher-voltage structure in the derivative curve at zero microwave power (see the -55-dB curve in Fig. 23) is presumably due to the interaction of the array with its cavity environment, such as it is. As the microwave power was increased this structure was suppressed. The number of correlated steps can clearly be seen to increase as the microwave power is built up. The voltage interval between these steps is accurately $4\hbar\omega/2e = 76$ μV for a microwave frequency of 9.1 GHz (equivalent to a Josephson voltage $\hbar\omega/2e = 19$ μV). This is clearly demonstrated in Fig. 24 which shows the initial buildup of the correlated steps at low rf power levels. At the highest power levels (~2 mW) over 100 correlated steps were counted. A typical derivative curve for high input powers is shown in Fig. 25.

One noticeable feature of these curves is that, unlike those for the square array, the first ($n=1$) correlated step is missing. This is shown very clearly in Fig. 26. Presumably, the way the array couples to the microwave field at low power levels depends on the geometry of the array. Certain geometries (viz., the square array) may be favored over others in forming a correlated state for weak synchronizing fields.

Obviously, no fully correlated steps will be observed at bias voltages $< M\hbar\omega/2e$. However, what happens in the voltage interval $0 < V < M\hbar\omega/2e$ presumably depends on the strength of the coupling of the individual junctions to the microwave field. At low power levels only one junction appears to be active in this voltage range since the minima are

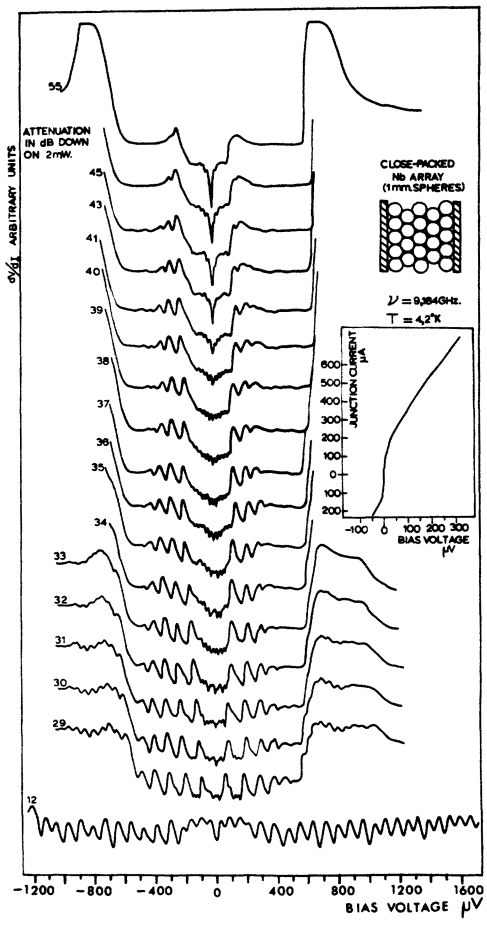

FIG. 23. Derivative curves for a close-packed (5 × 5) array of 1-mm Nb spheres at various levels of rf power. The minima in dV/dI vs V correspond to the current steps in I vs V. The junction I-vs-V curve at zero microwave power is shown inset.

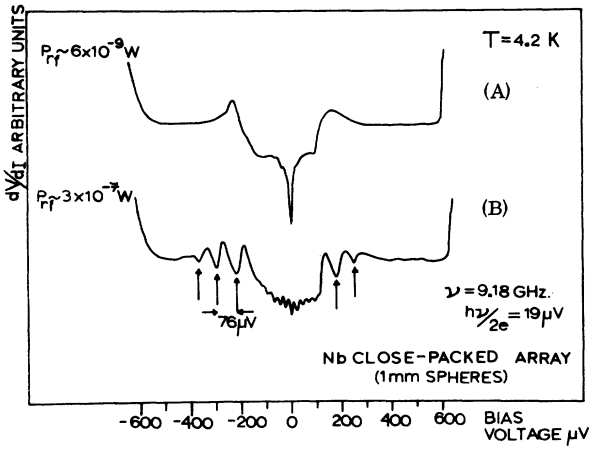

FIG. 24. Initial buildup of correlated steps at low rf power levels. Curve (B) was taken at −38-dB attenuation.

spaced at regular 20-μV intervals. The voltage-dependent transition from the uncorrelated to the correlated state can conceivably be though of as a phase transition.[60] At higher power levels three junctions seem to be coupled together in this critical region. Certainly, synchronization of the whole array is not complete until bias voltages well in excess of $M\hbar\omega/2e$ are reached. For comparison we present in Fig. 27 derivative curves for a close-packed array showing less than full correlation. The same $\hbar\omega/2e$ voltage spacing is seen between steps close to zero bias voltage. At higher voltages, partially correlated steps are induced, i.e., $V=3\hbar\omega/2e$. Figure 28(a) shows the I-vs-V characteristics of an even more weakly correlated square array, where $V=2\hbar\omega/2e$. For very inferior arrays just one weak link (or row of links) could be active. This is illustrated in Fig. 28(b) for a 5×5 square array.

From the evidence of the curves in Figs. 20, 23, 27, and 28, it seems certain that for particular ranges of microwave power and bias voltage, a perfect two-dimensional point-contact array can be driven into synchronization by an external microwave field. By perfect, we mean an array which by some route has four weak links available across the array between the electrodes. Probably, the same will be true of one- and three-dimensional arrays, provided good coupling can be arranged between the array and the microwave field.

At any given power the synchronizing effect of the microwave field might be expected to weaken for the highest-order steps since these involve nth order processes. That is to say, n photons at frequency ω mix with an ac Josephson current at frequency $n\omega$ to produce a current step at voltage $n\hbar\omega/2e$. We appear to have seen the effect of the weakening of the correlation across the array. In Fig. 29 there is a sudden change of step interval at large bias voltages from 76 to 57 μV. As the microwave power increased so the number of fully correlated steps increased; the "transition" region moved to higher bias voltages. At certain microwave power levels some of the derivative curves for the close-packed array of Fig. 23 showed transitions $4\rightarrow 3\rightarrow 2\rightarrow 1\,\hbar\omega/2e$ as the bias voltage was increased.

We also tried this synchronization with 4-mm radiation. The 4-mm system was coupled to the 3-cm cryostat waveguide by means of a 4-mm to 3-cm rectangular cross-section waveguide transition. Obviously, the 4-mm wave was multimoded in the oversized 3-cm guide. We might, therefore, expect a rather complicated interaction between the microwave field and the array. This was found to be the case.

Figure 30 shows structure induced in the dV/dI-vs-V curve of a 5×5 close-packed array of 1-mm niobium spheres (the derivative results in Figs. 23–26 are for the same array). There is a great wealth of detail at low bias voltages. Presumably, each mode can interact with the array separately. However, at higher voltages and over a restricted range of microwave power, the derivative curves appear to indicate full correlation across the array with a voltage interval between minima of 600 μV (i.e., almost exactly $4\hbar\omega/2e=582$ μV for $\nu=70.3$ GHz). It seems reasonable to assume that the strength of the coupling of the array to the 4-mm radiation field depends on the particular mode involved. For high-order steps, where n photons were involved, it may be that the mode best cou-

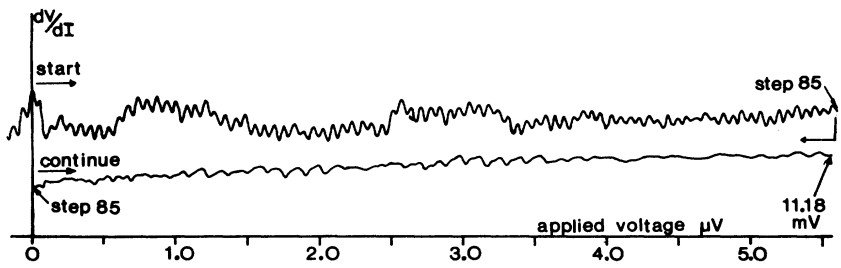

FIG. 25. Derivative curve for the array of Figs. 23 and 24 taken to high bias voltages. Microwave input power ~2 mW. For bias voltages >1 mV the array shows complex switching behavior between the fully correlated state ($V=4\hbar\omega/2e$) to the partially correlated state ($V=3\hbar\omega/2e$). Microwave-induced structure extends to at least 11 mV.

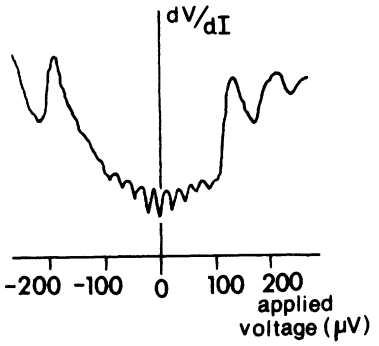

FIG. 26. Detail of the "single" quantum-voltage steps at small-bias voltages. The minima are at 20-μV intervals.

pled to the array dominates over all others, leading to simplified microwave-induced structure in dV/dI vs V.

It should be noted that at lower microwave power levels, both 3-cm and 4-mm radiation partially suppress the $n=0$ zero-voltage supercurrent. In this the array behaves like a single point-contact

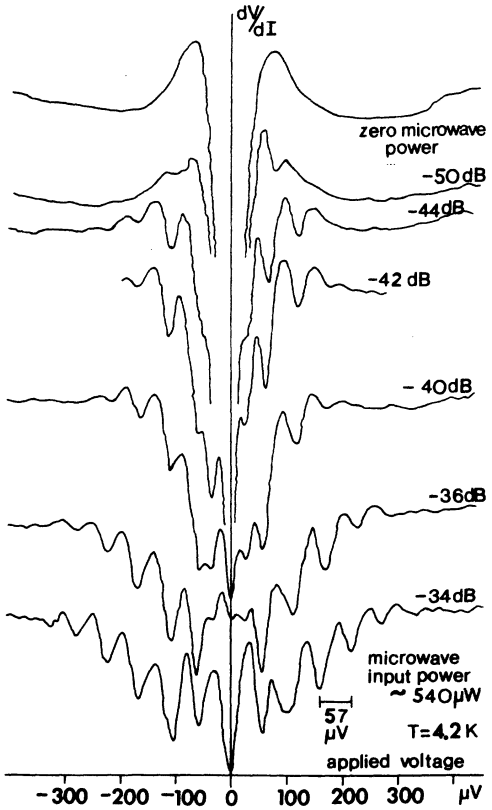

FIG. 27. dV/dI-vs-V curves at various levels of microwave power for a close-packed 5 × 5 array of 1-mm Nb spheres showing less than full correlation ($V = 3\hbar\omega/2e$).

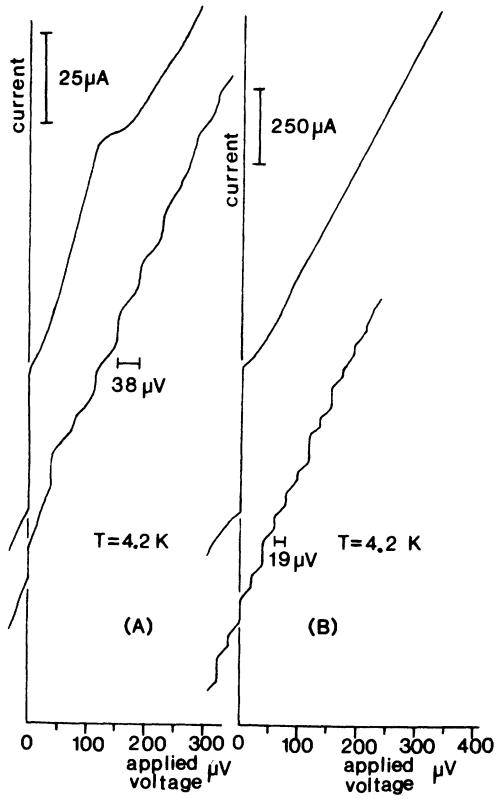

FIG. 28. (a) Partial correlation in a square array (5 × 5) of 1-mm Nb spheres; the current steps occur at intervals of $2\hbar\omega/2e$. (b) Single-voltage steps in a 5 × 5 Nb array at intervals of $\hbar\omega/2e$.

junction. We, therefore, assume that on the $n=0$ step the array behaves as a broadband detector of radiation.

VII. DETECTION OF MICROWAVES BY POINT-CONTACT JUNCTION ARRAYS

In order to evaluate point-contact arrays as broadband and narrow-band detectors of microwave radiation we used the previously mentioned techniques developed by Grimes *et al.*[51] and Richards and Sterling.[52] The broadband detection experiment involved monitoring the depression of the $n=0$ zero-voltage supercurrent peak. The X-band (3-cm) microwave system has already been referred to in Sec. VI. At $\nu = 9.188$ GHz, the total "insertion" loss of power from the output end of the ferrite isolator, to the array end of the cryostat waveguide was 3.4 dB at room temperature. The low-thermal-conductivity stainless-steel guide used in the cryostat was gold plated on the inside to cut down transmission losses. In our experiments, which all involved X-band radiation, the incident microwaves ($\nu = 9.188$ GHz) were modulated at 487 Hz. This frequency was chosen to keep clear of any harmonic frequency of the mains (at 50 Hz).

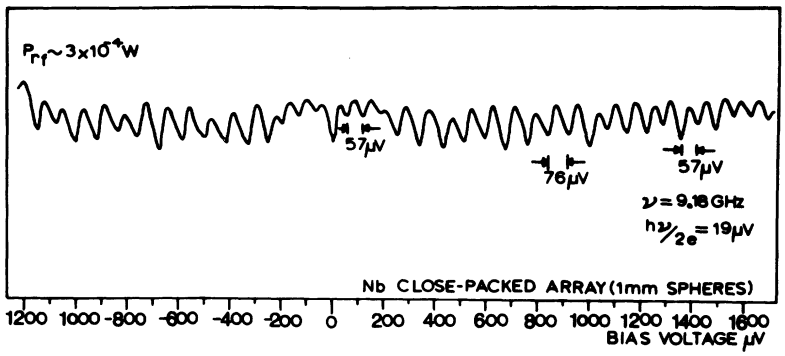

FIG. 29. Correlated steps for the close-packed array of Fig. 23 at relatively high rf power levels. Full correlation appears to break down on the high-order steps (at $V_{bias} \sim 1350$ μV).

With the microwave modulation turned on, the bias current through the array was swept slowly and the ac voltage developed across the array was detected with a PAR lock-in amplifier, model No. HR-8. This was used in conjunction with PAR type-B low-impedance preamplifier.

The rectified output from the PAR was plotted on an X-Y plotter as a function of bias current. Figure 31 shows the amplifier output plotted against bias current for a 5×5 square array of 1-mm Nb spheres at a temperature of 4.2 K. The array is swept from negative to positive polarity which accounts for the change in sign of the output on passing through the origin. Peaks (a) of Fig. 31 correspond to the maximum zero-voltage supercurrent flowing in the array. This is the broadband response of Grimes *et al.*[51] Between these two peaks the X-Y plotter is just recording the noise output from the amplifier. The maximum signal-to-noise ratio is ~70 for a peak-to-peak input power of 3×10^{-13} W. The structure beyond the zero-voltage supercurrent peaks appears to be rather complicated, but on cooling the array down to 2.45 K this degenerates into just one peak, as shown in Fig. 32. The signal to noise has improved to about 600. Also included in Fig. 32 are the relevant sections of the I-vs-V characteristics. The very noticeable depression in the $n=0$ step caused by the application of $\sim 3.5\times10^{-13}$ W of microwave power is accompanied by the decrease in amplitude of what must be assumed to be a cavity-induced bump in the characteristic.[52] This is illustrated very well in Fig. 33, which shows how the array response peak associated with the cavity-induced structure changes sign with decreasing microwave power.

Figure 33 shows the response curves for the array at 1×10^{-13}-W and 2×10^{-14}-W peak power. From the latter curve with a voltage signal to noise of 10, an amplifier (CR) time constant of 3 sec, and a 12-dB roll off on the PAR HR-8, the noise equivalent power (NEP), i.e., the microwave power which will produce a signal from the amplifier just equal to the noise signal, is found to be ~1 $\times10^{-14}$ W $(\mathrm{Hz})^{1/2}$. We have assumed an amplifier bandwidth of $2\pi CR$ (= 18.85 Hz) in this calculation. The response of a single junction biased onto the $n=0$ step should be inversely proportional to the square of the microwave frequency.[41] On the single-frequency argument at $\lambda = 4$ mm, the NEP of this array should be $\sim 5\times10^{-13}$ W $(\mathrm{Hz})^{1/2}$. We ignore any increase in response due to the Riedel-Werthamer peak in the ac current amplitude. This $\lambda = 4$-mm estimate is the same as that quoted by Grimes *et al.*[51] for a single Nb-Nb point-contact

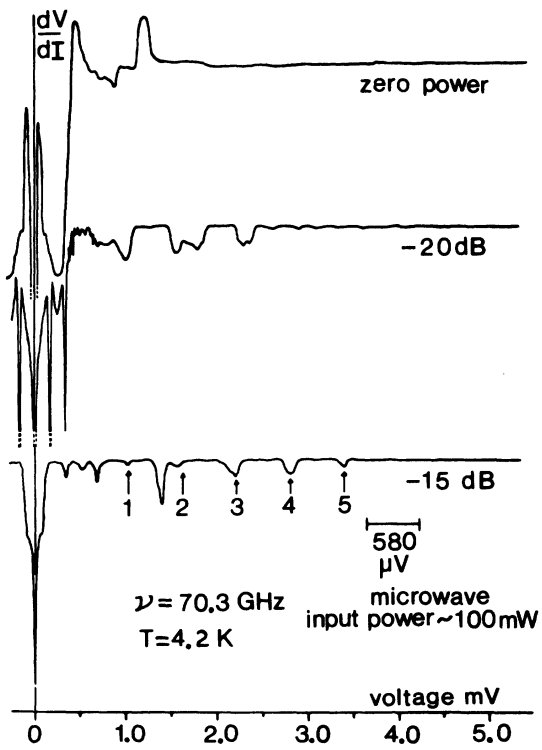

FIG. 30. dV/dI-vs-V curves for the array of Fig. 23 at various levels of E-band microwave power. The arrows 1–5 on the −15-dB curve are separated by 580 μV. Pronounced minima at voltage intervals of 145 μV ($=\hbar\omega/2e$) can be seen close to the voltage origin in the −20-dB curve.

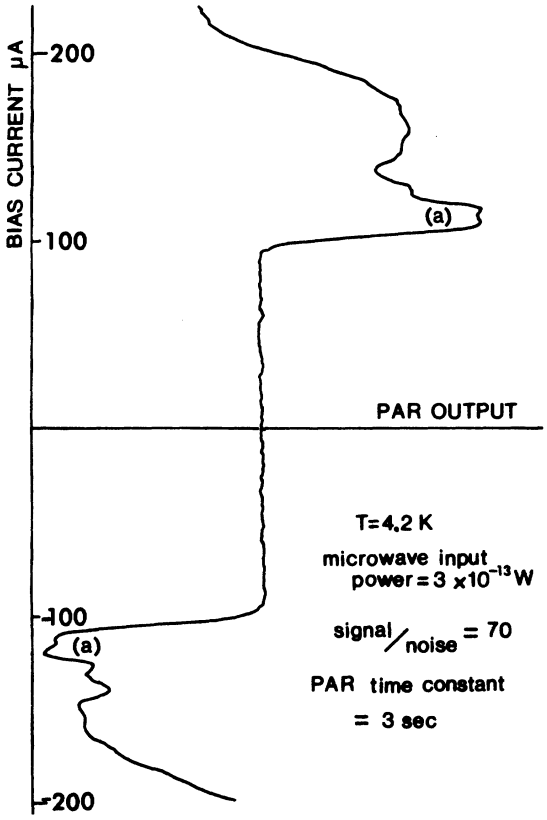

FIG. 31. X-band microwave response of 5×5 square array of 1-mm Nb spheres as a function of bias current. Peaks (a) correspond to the $n=0$ zero-voltage supercurrent step.

junction. Figure 34 shows the change in the $n=0$ broadband response of the array for small values of the microwave power.

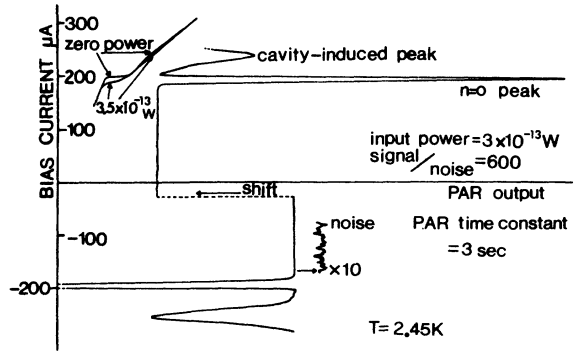

FIG. 32. X-band response for the 5×5 square array of Fig. 31 at $T=2.45$ K. For convenience response curve is shown shifted. The relevant section of the I-vs-V curve is also included. With the electrode contact resistance voltage subtracted the cavity-induced structure occurs at 127.5 μV (15.4 GHz on the single-frequency argument).

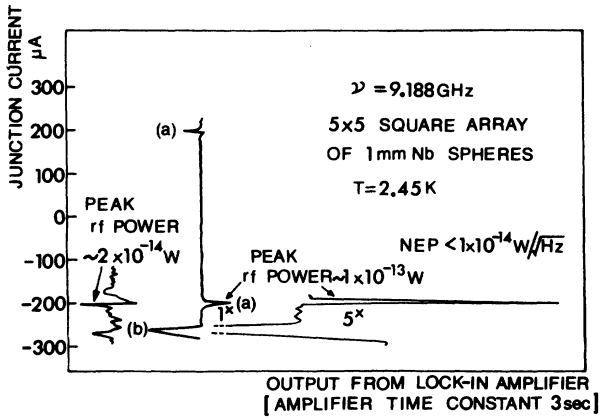

FIG. 33. X-band response of the Figs. 31 and 32 square array at very low microwave power levels. Estimated NEP $\lesssim 1\times10^{-14}$ W/(Hz)$^{1/2}$.

In Ref. 61 de Bruyn Ouboter *et al.* have demonstrated that a double point contact situated in a coaxial cavity can be "tuned" by means of an externally generated field. When the flux threading the hole between the contacts is equal to an integral number of flux quanta $n\Phi_0$, the supercurrents through the individual contacts oscillate with the same frequency and phase. Consequently, radiation is emitted. However, when the flux is equal to $(n+\frac{1}{2})\Phi_0$, the supercurrent through the two contacts oscillate with the same frequency but in opposite phase. The distance between the contacts is much less than the wavelength of the radiation; so with $\Phi=(n+\frac{1}{2})\Phi_0$ the net emitted radiation is very small. However, this experiment involved only

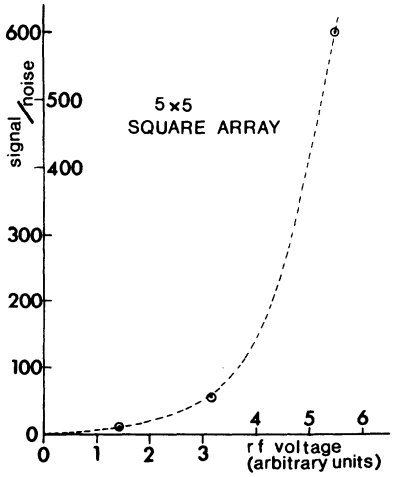

FIG. 34. Change in the $n=0$ zero-voltage supercurrent response (i.e., in terms of voltage signal to noise) as a function of rf voltage. Data taken from Figs. 32 and 33.

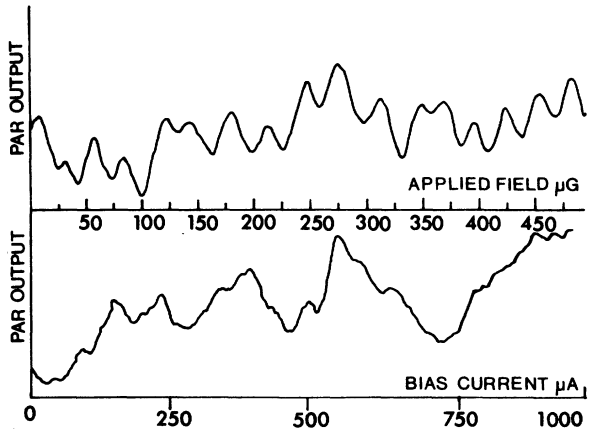

FIG. 35. (a) X-band response of square array biased onto a cavity-induced step as a function of the magnetic field generated by a Helmholtz pair. The field periodicity ΔH is 30.3 ± 3.58 μG; for a hole area between the weak links, $\simeq 0.25$ mm^2, $\Delta H = 25$ μG. (b) Drift of the X-band response over the same sweep time as in (a) but with the current now applied to an external resistor instead of the Helmholtz pair.

two weak links in parallel (i.e., feeding from two bulk superconducting reservoirs of phase ϕ_1 and ϕ_2).

Tilley[21] has pointed out that in a correlated array of weak links (one or two dimensional), the phase difference across each link adjusts so that the maximum power is radiated into the cavity. If this reasoning is correct, external magnetic fields should have little effect on cavity-induced structure in the I-vs-V characteristics of planar arrays.

To test this we current biased the array into the center of the "cavity" response peak in Fig. 33. A magnetic field perpendicular to the plane of the array could be generated by means of the Helmholtz pair already mentioned above. Figure 35 shows the result of plotting the PAR output as a function of field. The sweep time was 5 min. Figure 35(b) shows the drift on the PAR output over the same period of time with no magnetic field applied. It looks as if the "cavity" response is being modulated with a period of about 30 μG. This modulation is very weak, curves (a) and (b) of Fig. 35 being taken at 100× the amplification used in Fig. 33 (the modulation is about $\frac{1}{500}$th of the peak response).

The holes between the spheres in a square array of 1-mm spheres have cross-section areas of approximately 0.25 mm^2. For a two-junction interferometer with this enclosed area the field periodicity should be 10^{-4} G. For an $n = 5$ junction interferometer (see de Bruyn Ouboter *et al.*[61]) and, as before, an enclosed area for flux between contacts of 0.25 mm^2, the field periodicity should be $\frac{10}{4}^{-4} = 2.5 \times 10^{-5}$ G. This is apparently what we observe. However, since this modulation is so small compared to the size of the response peak, probably Tilley's phase-adjustment argument[21] is substantially correct.

It was not our intention to produce structure in the array characteristics by making the arrays interact with an external cavity. In fact, for the microwave-induced current-step experiments we would have preferred to have seen no self-induced structure at all. However, excess current bumps were observed in the characteristics of the arrays. For example, the rather weak-induced structure in curve (c) of Fig. 33 produces a large response at microwave power levels $\sim 1 \times 10^{-13}$ W. On one run with a 5×5 square array, what we suspected to be cavity-induced structure showed spectacular response to microwaves.

Curve (a) in Fig. 36 shows the response curve of the array as a function of the bias current at a micro wave power of 5×10^{-14} W. In this measurement the bias current was swept slowly from a very high-impedance current source (~ 1000 MΩ impedance). Unlike the previous response curves this one starts out at zero current. The small peak marked R_0 corresponds to the $n = 0$ step. The current-voltage characteristic is included to make this clear. The large peak marked R_c is the response peak referred to above. At this power level the signal-to-noise ratio is about 100. The response curve at the limit of attenuation available (2×10^{-14}-W microwave power p.t.p.) is shown in curve (b) of Fig. 36. The signal-to-noise ratio is here about 35. If we were to work out an NEP on this figure, given an amplifier time constant of 3 sec with a 12-dB roll off, we would arrive at a value of 2.5×10^{-15} W/(Hz)$^{1/2}$.

We are fairly confident that we were observing

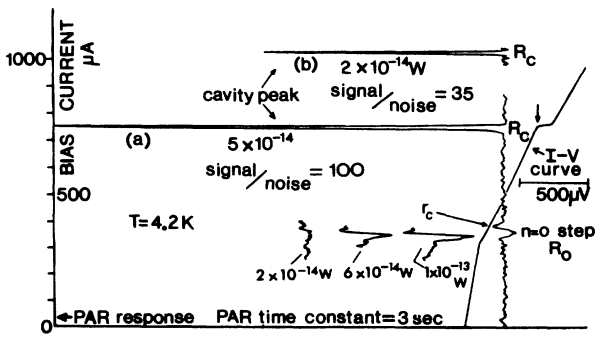

FIG. 36. X-band response of a 5× 5 array of 1-mm Nb spheres as a function of bias current. R_0 refers to the $n = 0$ zero-voltage supercurrent response, r_c is the response from weak cavity-induced structure, and R_c is the response from strong self-induced structure.

the response of a cavity-induced shouldered peak because the response of this peak to low power microwaves is of opposite sign to the response peak for the $n=0$ step. This is shown in Fig. 36 for various values of microwave power. Strong self-induced structure, although not as sharp as the shouldered peak described above, was frequently seen in the current-voltage characteristics of these 5×5 arrays. The above step corresponds to the 31.4-GHz structure shown in Fig. 4, after a correction for the electrode contact-resistance voltage has been made.

Tilley's theory[21] of correlated arrays introduces the concept of the super-radiant state in which the photon density in the cavity surrounding the array is proportional to the square of the number M of weak links in the array. Since the common photon field feeds back into the array, the amplitude of the self-induced current peak at the cavity voltage ($V=M\hbar\omega_c/2e$) is presumably also proportional to M^2. In narrow-band detection it is the height of cavity-induced peak which is monitored. We suggest that in arrays which are correlated the response (i.e., the change in height) of the self-induced peak at the cavity voltage will go as M^2. The number of weak links across the array between the electrodes is 20, therefore, $M^2=400$. Since we do not know the field patterns (i.e., the mode) close to the array we should take the upper limit for M as 40, the total number of weak links available in a perfect array. Hence, for a perfect array we might expect $400\leq M^2\leq1600$. Richards and Sterling[52] quote an NEP $\lesssim 1\times10^{-14}$ W/(Hz)$^{1/2}$ for a single Nb-Nb junction operating at a frequency of about 200 GHz ($V_c\simeq400$ μV). If we scale this value up by a factor of M^2, without concerning ourselves with the Riedel–Werthamer singularity at $2\Delta/e$ [given that 400 $\mu V\ll 2\Delta(\mathrm{Nb})/e\simeq3$ mV],[62] we find an NEP in the range $(1-5)\times10^{-16}$W/(Hz)$^{1/2}$ This is comparable with the value calculated above for the square array. We have, of course, assumed the coupling of the radiation to both single junction and array to be the same. Considerable improvement in NEP may well be achieved by situating the array in a well-defined microwave cavity. Also from the super-radiance argument, increasing the number of weak links in the array should have a marked effect on its narrow-band detection capabilities.

In the above discussion we have assumed implicitly that the array is coupled to the radiation via the E field. However, an array of point contacts can be regarded as a set of coupling loops. It is conceivable, therefore, that the array would prefer to couple to the H rather than the E component of the electromagnetic field. A simple Josephson interferometer, consisting of two weak links in parallel, can, under suitable operating conditions, attain a magnetic field sensitivity of $\sim10^{-10}$ G. A magnetometer of this sensitivity should, according to Richards,[41] have a microwave power sensitivity, in the millimeter region of the spectrum, of approximately 4×10^{-20} W/(Hz)$^{1/2}$, for a loop area equal to 1 mm^2. In Ref. 61 de Bruyn Ouboter *et al.* have derived an expression for the maximum supercurrent I_{max} which can pass through an N-junction Josephson interferometer with all the junctions equally spaced. They find that if self-inductances and mutual inductances of the holes between the contacts are neglected, the expression for I_{max} is of the form

$$I_{max}=I_0\left|\frac{\sin N\pi\Phi/\Phi_0}{\sin\pi\Phi/\Phi_0}\right|,$$

where Φ is the flux threading each hole between the contacts, and Φ_0 is the flux quantum $=hc/2e$ $=2.07\times10^{-7}$ G cm^2.

The measurement of magnetic field H by a Josephson interferometer consists of detecting the change in I_{max} as the field is varied. Obviously, for an N-junction system the response dI_{max}/dH is greatest on the downward slopes of the principal maxima. The response increases roughly as $\frac{1}{2}N$. Now a system of N Josephson junctions in parallel is analogous to the N-slit diffraction grating in optics or the linear array of N dipoles in antenna theory. However, this analogy cannot be extended to two dimensions; a two-dimensional array of Josephson junctions will still have a response which is proportional to N. This is in contrast to a stacked broadside array of $N\times N$ dipoles where the forward power gain is enhanced by a factor of N^2 over a single dipole.

For example, judged as a magnetometer, a 5×5 square array of 1-mm niobium spheres should have a microwave power sensitivity of $\sim1\times10^{-19}$W/(Hz)$^{1/2}$. This order-of-magnitude calculation assumes, of course, that the intrinsic noise in such arrays is not the limiting factor.[63]

VIII. CONCLUSIONS

We have attempted in this work to offer experimental proof of the existence of a "correlated" state in arrays of point-contact Josephson junctions. Thus the Fabry–Perot experiments described in Sec. IV suggest very strongly that an array, when voltage biased close to a cavity resonance frequency, can enter a single-frequency state in which the voltage drops across all the junctions in the array are equal. However, this straightforward description of the mode of operation of our point-contact arrays is obviously not complete. The voltage at which self-induced structure in I vs V occurs is observed to increase as the temperature is decreased below the superconducting transition temperature of the array. The

mechanism responsible for this shift is still a matter for speculation. Additional qualitative support for this correlated state is provided by the transmitter-detector experiments. Observed power levels and upper-frequency limits seem difficult to account for without invoking the single-frequency condition. We have, of course, been helped very considerably in the interpretation of our results by Tilley's theory of super-radiance[21] in arrays of weak links.

Recently, Finnegan and Wahlsten[64] have provided elegant proof of the super-radiant state in the simplest possible array system—viz., two tunnel-oxide Josephson junctions connected in series. Such coupled systems obviously hold promise as low-power sources in the millimeter and submillimeter regions of the spectrum. Earlier experiments on point-contact tin-sphere arrays,[43] where power-level changes $\sim 10^{-5}$ W were observed, indicate that coupled arrays with milliwatt power outputs may eventually be realized. Microwave harmonic conversion[65] and parametric amplification[1] are obvious but potentially fruitful applications of weak-link arrays.

The microwave experiments described in Sec. VI demonstrate very convincingly that small arrays at least can be driven into collective synchronization by weak microwave fields. There now seems to be some experimental evidence that such synchronization is possible in large scale arrays of weak links.[4] One interesting feature of these microwave experiments which might repay further study is the voltage-controlled phase transition which appears to take place between the uncorrelated and correlated states.

Further work should obviously be directed towards exploring the dc state of weak-link arrays, particularly in the light of Rosenblatt's interesting analogies[26] with spin-ordered systems. In addition the narrow-band detection capabilities of weak-link arrays have, as yet, only been superficially investigated.

ACKNOWLEDGMENTS

I should like to offer my thanks to Dr. D. R. Tilley for his invaluable support, to Professor J. Volger for his able guidance during my stay at the Philips Laboratories, and particularly to Professor W. W. Webb for providing me with the opportunity to take up this work again through ONR Grant No. N00014-67-A-0077-0016. I should also like to thank Dr. J. Kurkijärvi of Cornell University and Dr. M. Strongin and his colleagues at the Brookhaven Laboratory for recent interesting discussions.

[1]H. Zimmer, Appl. Phys. Lett. **10**, 193 (1967); see also, A. S. Clorfeine, Appl. Phys. Lett. **4**, 131 (1964).
[2]R. H. Parmenter, Phys. Rev. **154**, 353 (1967); Phys. Rev. **167**, 387 (1968).
[3]C. A. Neugebauer and M. W. Webb, J. Appl. Phys. **33**, 74 (1962).
[4]A. Saxena, J. E. Crow, and M. Strongin, in Proceedings of the Thirteenth International Conference on Low Temperature Physics, Boulder, Colo., 1972 (unpublished).
[5]I. Warman, M. T. Jahn, and Y. H. Kao, J. Appl. Phys. **42**, 5194 (1971).
[6]P. W. Anderson, Prog. Low Temp. Phys. **5**, 40 (1967).
[7]S. Shapiro, Phys. Rev. Lett. **11**, 80 (1963).
[8]A. H. Dayem and J. J. Weigand, Phys. Rev. **155**, 419 (1967); see also, A. F. G. Wyatt, V. M. Dmitriev, W. S. Moore, and F. W. Sheard, Phys. Rev. Lett. **16**, 1166 (1966).
[9]A. T. Fiory, Phys. Rev. Lett. **27**, 501 (1971).
[10]T. D. Clark and D. R. Tilley, Phys. Lett. A **28**, 62 (1968).
[11]L. Bragg and J. F. Nye, Proc. R. Soc. Lond. **190**, 474 (1947).
[12]J. E. Bolton and D. H. Douglass, Jr., Solid State Commun. **9**, 2263 (1971).
[13]A. Longacre and S. Shapiro, Bull. Am. Phys. Soc. **II16**, 399 (1971).
[14]B. N. Taylor, J. Appl. Phys. **39**, 2490 (1968).
[15]J. D. Krauss, *Atennas* (McGraw-Hill, New York, 1950), p. 222.
[16]D. E. McCumber, J. Appl. Phys. **39**, 297 (1968).
[17]J. E. Zimmerman, *Recent Developments in Superconducting Devices*, Nat. Bur. of Std. Rept. No. COM-71-00808 (U. S. GPO, Washington, D.C., 1971).
[18]A. H. Dayem and C. C. Grimes, Appl. Phys. Lett. **9**, 47 (1966).
[19]E. V. D. Glazier and H. R. L. Lamont, *Transmission and Propagation* (Her Majesty's Stationary Office, London, 1958), p. 257.
[20]A. J. DiNardo, J. G. Smith, and F. R. Arams, J. Appl. Phys. **42**, 186 (1971).
[21]D. R. Tilley, Phys. Lett. A **33**, 205 (1970).
[22]R. H. Dicke, Phys. Rev. **93**, 99 (1954).
[23]A. L. Schawlow and C. H. Townes, Phys. Rev. **112**, 1940 (1955).
[24]H. Cortès, P. Pellan, and J. Rosenblatt, in *Proceedings of the Twelfth International Conference on Low Temperature Physics* (Keigaku, Tokyo, 1970), p. 487.
[25]P. Pellan, G. Dousselin, H. Cortés, and J. Rosenblatt, Solid State Commun. (to be published).
[26]J. Rosenblatt, Solid State Commun. (to be published).
[27]T. D. Clark and D. R. Tilley, Phys. Lett. A **29**, 514 (1969).
[28]S. F. Strait, M. S. thesis (Cornell University, 1971) (unpublished).
[29]A. Hadni, *Essentials of Modern Physics applied to the Study of the Infrared* (Pergamon, New York, 1967).
[30]V. Ambegaokar and A. Baratoff, Phys. Rev. Lett. **10**, 486 (1963); Phys. Rev. Lett. **11**, 104 (1963).
[31]N. V. Zavaritskii, Zh. Eksp. Teor. Fiz. **43**, 1123 (1962) [Sov. Phys.-JETP **16**, 793 (1962)].
[32]J. M. Rowell and W. L. Feldman, Phys. Rev. **172**, 394 (1968).
[33]N. R. Werthamer and S. Shapiro, Phys. Rev. **164**, 523 (1967).
[34]J. I. Pankove, Phys. Lett. **21**, 406 (1966); Phys. Lett. **22**, 557 (1966).
[35]J. E. Zimmerman and A. H. Silver, Phys. Rev. **141**, 367 (1966).
[36]E. A. Lynton, *Superconductivity* (Methuen, London, 1962),

p. 37.
[37]E. A. Lynton, in Ref. 36, p. 40.
[38]D. E. McCumber, J. Appl. Phys. **40**, 3113 (1968).
[39]J. Clarke and T. A. Fulton, J. Appl. Phys. **40**, 4470 (1969).
[40]H. A. Atwater, *Introduction to Microwave Theory* (McGraw-Hill, New York, 1962), p. 222.
[41]P. L. Richards, *Physics of III-V Compounds* (Academic, New York, 19XX), Vol. 6.
[42]B. T. Ulrich and E. O. Kluth, in Proceedings of the Applied Superconductivity Conference, Annapolis, Md., 1972 (unpublished).
[43]T. D. Clark, Phys. Lett. A 27, 585 (1968).
[44]D. J. Repici, L. Leopold and W. D. Gregory, in Ref. 42.
[45]E. Riedel, Z. Naturforsch. A **19**, 1634 (1964).
[46]N. R. Werthamer, Phys. Rev. **147**, 255 (1966); see S. A. Buckner, T. F. Finnegan, and D. N. Langenberg [Phys. Rev. Lett. **28**, 150 (1972)] for experimental data.
[47]J. Barden, L. N. Cooper, and J. R. Schrieffer, Phys. Rev. **108**, 1175 (1957).
[48]B. W. Roberts, Superconducting Materials and Some of Their Properties, G. E. Res. Report No. 61-RL-2744M, June, 1961 (unpublished).
[49]T. D. Clark, in Proceedings of the Conference on Science of Superconductivity, Stanford, 1969 (ubpublished); Physica (Utr.) **55**, 432 (1971).
[50]C. C. Grimes, P. L. Richards, and S. Shapiro, Phys. Rev. Lett. **17**, 431 (1968).
[51]C. C. Grimes, P. L. Richards, and S. Shapiro, J. Appl. Phys. **39**, 3905 (1968).
[52]P. L. Richards and S. A. Sterling, Appl. Phys. Lett. **14**, 394 (1969).
[53]B. D. Josephson, Phys. Lett. **1**, 251 (1962).
[54]T. D. Clark, in Ref. 24, p. 449.
[55]W. H. Parker, D. N. Langenberg, A. Denenstein, and B. N. Taylor, Phys. Rev. **177**, 639 (1969).
[56]M. J. Stephen, Phys. Rev. **186**, 393 (1969).
[57]P. E. Gregers-Hansen, M. T. Levinsen, and G. Fog Pedersen, J. Low Temp. Phys. **7**, 99 (1972).
[58]P. Russer, Acta Phys. Austriaca **32**, 373 (1970).
[59]H. Fack and V. Kose, J. Appl. Phys. **42**, 320 (1971).
[60]J. Crow and M. Strongin (private communication).
[61]R. De Bruyn Ouboter and A. Th. A. M. DeWaele, Prog. Low Temp. Phys. **6**, 273 (1970).
[62]P. G. de Gennes, *Superconductivity of Metals and Alloys* (Benjamin, New York, 1966), p. 10.
[63]J. Kurkijärvi and W. W. Webb, in Ref. 42.
[64]T. Finnegan and S. Wahlsten, in Ref. 4.
[65]S. Shapiro, J. Appl. Phys. **38**, 1879 (1967).

PHYSICAL REVIEW B VOLUME 8, NUMBER 1 1 JULY 1973

Magnetic Measurements on Strong-Coupling $Pb_{1-2x}Bi_xTl_x$ and Pb-In Superconducting Alloys*

J. H. Fearday† and R. W. Rollins
Department of Physics, Ohio University, Athens, Ohio 45701
(Received 25 September 1972)

Measurements are presented of the generalized Ginzburg-Landau parameter $\kappa_2(T)$ and the bulk upper-critical field $H_{c2}(T)$ as a function of temperature T near the critical temperature in $Pb_{1-2x}Bi_xTl_x$, where $x = 0.015$, 0.05, 0.10, and 0.15, and of $H_{c2}(T)$ in Pb_{1-y} In_y, where $y = 0.018$, 0.53, 0.087, and 0.167. These results, and previous measurements of κ_2 in Pb-In by Farrell *et al.*, which are in disagreement with weak-coupling theories are found to be in ageement with calculations by Eilenberger and Ambegaolar and by Usadel which include both strong-coupling and electron-mean-free-path effects.

I. INTRODUCTION

We present in what follows measurements of the generalized Ginzburg-Landau[1-4] parameter κ_2 and the upper-critical field H_{c2} as a function of temperature for some Pb alloys for which the electron-phonon coupling is too strong to be treated by the weak-coupling extensions[2,3] of the Bardeen-Cooper-Schrieffer (BCS)[5] theories. The measurements are shown to be in general agreement with recent calculations, which include both strong-coupling and electron-mean-free-path effects, by Elienberger and Ambegaokar[6] and by Usadel.[7]

Elienberger and Ambegaokar have shown that when calculating $(dH_{c2}/dT)_{T_c}$, the effects of strong-coupling and of electron mean free path may be factored. The strong-coupling factor does not depend explicitly on the mean free path and is expressed in terms of the thermodynamic critical field $H_c(T \to T_c)$ and the energy-gap parameter $\Delta(T \to T_c)$, which may be obtained from experiment. Usadel has shown a similar strong-coupling factor exists for $\kappa_2(T_c)$ in the dirty limit.

The Pb-Bi-Tl system was chosen for several reasons: (a) Disordered substitutional alloys having the Pb crystal structure exist over a wide range of compositions, simplifying sample preparation; (b) all the constituents have nearly the same mass and, therefore, changes in the phonon spectrum and electron-phonon coupling due to ionic-mass changes should be minimized; (c) the $Pb_{1-2x}Bi_xTl_x$ system has a constant electron-to-atom ratio of 4, thus creating a system of "artifical lead" with essentially constant phonon spectrum and constant electron-gas density, giving rise to a constant electron-phonon coupling for the entire system; (d) tunneling measurements have been reported by Dynes and Rowell[8] for $Pb_{1-2x}Bi_xTl_x$ alloys.